



RESEARCH ARTICLE

10.1029/2018JC013832

Comparative Effects of Climate Change and Tidal Stream Energy Extraction in a Shelf Sea

Key Points:

- Tidal energy extraction and climate change affect tidal elevation, currents, and ocean stratification
- Climate change effects on ocean stratification are 10 times larger than energy extraction effects
- Numerical simulations of the present and future hydrodynamics of the NW European continental shelf are presented

Supporting Information:

- Supporting Information S1

Correspondence to:

M. De Dominicis,
micdom@noc.ac.uk

Citation:

De Dominicis, M., Wolf, J., & O'Hara Murray, R. (2018). Comparative effects of climate change and tidal stream energy extraction in a shelf sea. *Journal of Geophysical Research: Oceans*, 123, 5041–5067. <https://doi.org/10.1029/2018JC013832>

Received 25 JAN 2018

Accepted 14 JUN 2018

Accepted article online 26 JUN 2018

Published online 30 JUL 2018

Michela De Dominicis¹ , Judith Wolf¹, and Rory O'Hara Murray² ¹National Oceanography Centre, Liverpool, UK, ²Marine Scotland Science, Scottish Government, Aberdeen, UK

Abstract The environmental implications of tidal stream energy extraction need to be evaluated against the potential climate change impacts on the marine environment. Here we study how hypothetical very large tidal stream arrays and a *business as usual* future climate scenario can change the hydrodynamics of a seasonally stratified shelf sea. The Scottish Shelf Model, an unstructured grid three-dimensional ocean model, has been used to reproduce the present and the future state of the NW European continental shelf. Four scenarios have been modeled: present conditions and projected future climate in 2050, each with and without very large scale tidal stream arrays in Scottish Waters (UK). It is found that where tidal range is reduced a few centimeters by tidal stream energy extraction, it can help to counter extreme water levels associated with future sea level rise. Tidal velocities, and consequently tidal mixing, are also reduced overall by the action of the tidal turbine arrays. A key finding is that climate change and tidal energy extraction both act in the same direction, in terms of increasing stratification due to warming and reduced mixing; however, the effect of climate change is an order of magnitude larger.

Plain Language Summary Tidal currents can turn underwater turbines, which can generate electricity. Tides in Scotland (United Kingdom, UK) can provide 10% of the present UK electricity demand. Does this come without side effects on the marine environment? The answer is no, but those side effects are going to be local and much smaller than the effects of climate change. We do not have a time machine, but we can use a numerical ocean model, a computer software that is able to predict the movement of ocean currents, among other things. We can simulate the present and future conditions in 2050 of the North and Irish Seas, with and without the ocean bottom being covered in some areas with underwater turbines. Our predictions tell us that the underwater turbines will slow down the ocean currents. This leads to a less vertical mixing of the ocean, reducing the exchange of water between the ocean bottom and the surface. However, the ocean model also anticipates that global warming will have the same effect, but 10 times larger. We discovered that the underwater turbines can also change the sea level, and, in some situations, this can help to protect the coast against future sea level rise.

1. Introduction

It is now widely recognized that there is a pressing need to mitigate the effects of anthropogenically induced climate change and other environmental impacts of worldwide reliance on fossil fuels. The actions to be taken to achieve a reduction of greenhouse gas (GHG) emissions, and consequently the global mean temperature, include reducing emissions from the power sector and encouraging investment in low-carbon technologies by reforming the electricity market. The IPCC AR4 (Intergovernmental Panel on Climate Change Fourth Assessment Report, Solomon et al., 2007) was a key piece of evidence in setting the European Union's 2050 target to cut GHG emissions to 80%–95% below 1990 levels by 2050 (European Commission, 2011). The more recent IPCC AR5 (Fifth Assessment Report, Stocker et al., 2013) brought even more certainty in these conclusions and *well below 2°C above preindustrial levels* is the global temperature warming limit to which over 160 governments around the world have signed up with the Paris Agreement in 2015.

This widespread concern has led to a growing interest in alternative energy sources. The first generation of renewable energy technologies, such as solar and wind, are now available worldwide at commercially competitive prices. However, there is a pressing need to further diversify the low-carbon generation capacity and more attention is being focused on the untapped source of energy from the marine environment. Ocean energy technologies (including tidal, wave, and thermal) can be the next generation of renewable

©2018. The Authors.

This is an open access article under the terms of the Creative Commons Attribution License, which permits use, distribution and reproduction in any medium, provided the original work is properly cited.

energy, which will be needed if we are to meet the 2050's objective of reducing GHG emissions. Tidal stream energy extraction technology is currently more mature than wave or thermal technologies, and there are more developers at full-scale demonstration stage. The tidal energy sector has made significant progress toward commercialization in the UK, with the installation of the first tidal energy arrays in the Shetland Islands and the Pentland Firth. A number of smaller tidal projects have also gone live in the European Union and in Canada (Ocean Energy Systems, 2016). Those developments will lead the way for a group of coastal states, including China, Japan, South Korea, Australia, New Zealand, and Chile, that potentially could harness the power of their local tides.

Many of the environmental problems the world faces today, including climate change, air pollution, oil spills, and acid rain, result from worldwide reliance on fossil fuels; however, since we need energy and there is an impact no matter how we generate it, the objective is to minimize it both locally and globally. Extracting energy from the ocean leaves less energy in the ocean system, which will also have environmental impacts. The ecological implications of marine renewable energy extraction need to be considered and evaluated against the possibly greater and global ecological threat of anthropogenically induced climate change and other environmental impacts of the dependence on fossil fuels. In this context, the EcoWatt2050 project has been specifically designed to determine ways in which marine spatial planning and policy development can enable the maximum level of marine energy extraction while minimizing environmental impacts. The present paper is focused on tidal stream energy extraction and addresses the following questions: (i) How can marine energy developments affect ocean hydrodynamic processes that can be relevant for ecosystem habitats and animals' behavior? (ii) How can we differentiate the effects of climate change from energy extraction? (iii) Are there ways in which the deployment of marine renewables may ameliorate or exacerbate the predicted effects of climate change? The results presented in this paper are now being used by further studies to understand how the physical changes will translate into impacts on ecosystem habitats and animals' behavior.

Observations of the effects of energy removal by large-scale tidal stream arrays are not going to be possible until commercial-scale arrays have been deployed and operated for several years. Hydrodynamic models are therefore the best tool to estimate how tidal stream turbines may influence flow conditions. Evaluating the possible impacts might help facilitate the exploitation of tidal energy by scaling and locating planned tidal energy farms to minimize harm to the marine environment. Furthermore, putting those impacts in the context of the effects due to future climate change can help in better shaping marine policies related to tidal energy developments. To date, only a few studies (De Dominicis et al., 2017; Hasegawa et al., 2011; Karsten et al., 2008; van der Molen et al., 2016) have focused on very far-field (>100 km) environmental effects of energy removal by tidal stream turbines in different world locations. Among those, only van der Molen et al. (2016) and De Dominicis et al. (2017) have included atmospheric, oceanic, and riverine forcing in the model setup, which permits the study of impacts not only on the tidal dynamics but also on temperature, salinity, stratification, and residual ocean circulation. This is crucial, since these are the variables that affect the ocean ecosystems and habitat (Holt et al., 2012; Sadykova et al., 2017; Scott et al., 2010, 2013; Wakelin et al., 2015) and are also going to be modified by future climate conditions in the NW European continental shelf. Coherent findings in the climate change literature for the region include overall increases in sea level and ocean temperature, and a freshening of the North Sea, which lead to changes in stratification and residual circulation (Ådlandsvik, 2008; Holt et al., 2010; Mathis & Pohlmann, 2014; Mathis et al., 2017; Schrum et al., 2016; Tinker et al., 2016).

The above mentioned studies looked at the effects of both climate change and tidal energy extraction; however, none of those aimed to examine to the combined effects of climate change and energy extraction and to compare and differentiate their impacts. Therefore, the aim of this work is to examine the ocean response to both very large tidal stream turbine arrays in Scottish Waters and worst case future climate change conditions. A typical annual cycle of the present NW European continental shelf hydrodynamics was modeled and compared with output for the same period of time perturbed by very large-scale tidal stream energy extraction developments. In order to determine if the latter may ameliorate or exacerbate the effects of future climate change on the marine system, the hydrodynamic conditions representative of the projected future climate in 2050 were modeled, including two scenarios, one without tidal energy extraction devices and a second with plausible very large scale tidal stream array layouts. This allows us to evaluate the potential effect of climate change on the hydrodynamics and compare it with the future state of the seas modified by large-scale energy extraction.

The paper is organized as follows: section 2 presents the methodology to design (i) the tidal turbine arrays and (ii) the present and future climate model runs; section 3 presents the results, in terms of estimate of (i) power available from Scottish Waters and (ii) impacts on marine hydrodynamics of both tidal energy extraction and climate change; section 4 discusses the major outcomes and also limitations and future expected work, and section 5 highlights our conclusions.

2. Methodology

An unstructured grid coastal ocean model, FVCOM (Finite-Volume Community Ocean Model, Chen et al., 2003), was used to describe the hydrography and circulation of the Scottish continental shelf waters, using an implementation known as the Scottish Shelf Model (SSM, Wolf et al., 2016). The model domain includes the NW European continental shelf and extends beyond the shelf to include some of the adjacent northeast Atlantic deep waters (see supporting information for the model bathymetry and full domain). It has a variable horizontal resolution, with horizontal node to node spacing ranging from 10 to 20 km offshore down to 500 m–1 km near the coast. The horizontal grid is mainly refined in the water less than 200 m deep, that is, on the continental shelf (see supporting information for the spatial distribution of the mesh size). The model mesh has been built starting from the Global Self-consistent, Hierarchical, High-resolution Shoreline (GSHHS, <https://www.ngdc.noaa.gov/mgg/shorelines/gshhs.html>) data for the coastline. For the vertical discretization FVCOM uses a σ coordinate system (terrain following coordinates), and the SSM implementation has 20 uniform layers. The SSM model bathymetry was supplied by the European Marine Observation and Data Network (EMODnet, <http://www.emodnet-bathymetry.eu/>) and by the Northwest shelf Operational Oceanographic System (NOOS, <http://www.noos.cc/>), the latter for the North Sea east of 0°E. The time step is 3 s for the external mode (barotropic) and 18 s for the internal mode (baroclinic), as the governing equations can be solved in FVCOM using a split-mode method. The SSM uses the ability of FVCOM of solving the equations directly in spherical coordinates, which is important for basin or larger-scale ocean application.

The SSM has been used (i) to design the large theoretical arrays of tidal stream turbines, following a methodology described in section 2.1; (ii) to reproduce present and future ocean conditions in the NW European continental shelf, as described in sections 2.2 and 2.3; (iii) to estimate the maximum available power for electricity generation from Scottish Waters, presented in section 3.1; (iv) to evaluate the tidal energy extraction far-field effects during different seasonal and climatic conditions, shown in section 3.2.

2.1. Very Large Scale Tidal Turbine Arrays Design

Areas where tidal stream energy developments should be deployed to minimize the impact to the environment and to be sustainable and economically viable to Scotland were identified by the Scottish Government (The Scottish Government, 2015) from an analysis of different users of the sea (fishing, oil and gas, marine protected areas, recreation, etc.). The 10 *tidal plan option* sites are delimited by green lines in Figure 1 and are the locations of the tidal stream arrays designed in this work. They can be classified into three main regions: (1) the Pentland Firth and Orkney Waters (PFOW), which include the Pentland Firth, Westray, Eday, and Sanday; (2) the Shetland Islands, to which Sumburgh, Yell Sound, and Muckle Flugga belong; and (3) the west coast of Scotland, that comprises South West Islay, Solway Firth, and Mull of Kintyre.

The average power density (APD) in Scottish Waters is also shown in Figure 1. APD is the power density in a vertical plane perpendicular to the tidal current direction, defined as

$$APD(i) = \left\langle \frac{1}{2} \rho \overline{|\mathbf{u}(i, t)|^3} \right\rangle_t \quad (1)$$

where ρ is the water density, $\overline{|\mathbf{u}(i, t)|}$ is the depth-averaged tidal current speed, $\langle \rangle_t$ stands for time-averaging over 30 days. APD has been estimated from a 30-day tide-only run of SSM forced by eight tidal constituents ($M_2, S_2, N_2, K_2, K_1, O_1, P_1,$ and Q_1), obtained from the TPXO7.2 model, the Oregon State University tidal inversion model of TOPEX/POSEIDON altimeter data (Egbert & Erofeeva, 2002). Highest average power density areas are located in the PFOW, the Shetland Islands, and the west coast of Scotland regions and are indeed in agreement with the areas identified for tidal energy developments.

Starting from the 10 tidal plan option sites, large theoretical arrays of tidal stream turbines have been designed, which means identifying where and how many turbines should be deployed within those wider areas. The very large scale EcoWatt2050 tidal stream energy arrays for Scottish waters have been designed following a general method that considers three simple limitations: (i) a minimum water depth, 27.5 m; (ii) a

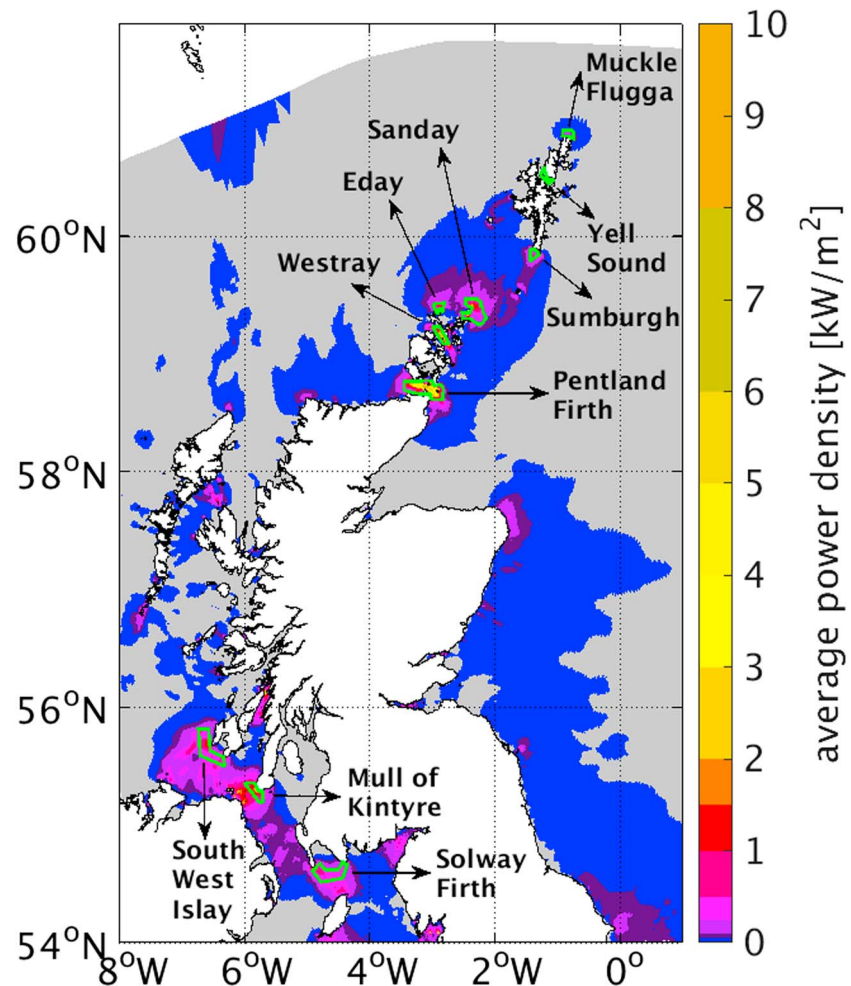


Figure 1. Average power density [kW/m^2] in Scottish Waters estimated from a 30-day Scottish Shelf Model run forced by eight tidal constituents (M_2 , S_2 , N_2 , K_2 , K_1 , O_1 , P_1 , and Q_1), without including any feedbacks of tidal arrays on the flow. Green lines indicate areas identified for exploitation.

turbine spacing limitation of 3×15 device widths; (iii) a capacity factor limit of 35%, following De Dominicis et al. (2017). The water depth limitation is driven by the choice of bottom-mounted horizontal axis turbines, not a particular design, but a generic one, as described in Baston et al. (2015), with 20-m diameter blades, which *weathervanes* into the tidal flow. The hub height has been set to be 15 m above the bed, giving a total height of 25 m. The turbine spacing is required to eliminate wake effects (Myers & Bahaj, 2010), giving a minimum lateral spacing of three device widths and a minimum downstream spacing of 15 device widths. The capacity factor (Polagye & Thomson, 2013; Robins et al., 2015) is defined as the ratio of the APD to the power density at the turbine-rated speed, $|\mathbf{u}_R(i)|$:

$$CF(i) = \frac{\left\langle \frac{1}{2} \rho |\mathbf{u}(i, t)|^3 \right\rangle_t}{\frac{1}{2} \rho |\mathbf{u}_R(i)|^3} 100 \quad (2)$$

In other words, the capacity factor is the ratio between the average instantaneous power and the maximum power (rated capacity) that can be generated by a turbine. Feasibility studies suggest a capacity factor in the range 30%–40% for the lowest cost of tidal stream energy (Bedard et al., 2006). The rated speed is the current speed at which the turbine reaches its maximum efficiency; when it is exceeded, the power output reaches the limit that the electrical generator is capable of. The rated speed (and turbine design) should be tuned (chosen) on the basis of the tidal regime in a particular site and within the limitations imposed by the turbine design (its electrical generator and structure). In this work, we assumed the tidal turbines could have a rated capacity of between 0.3 MW and 1 MW, that is, with a rated speed in the range 1.25–2 m/s. For less energetic

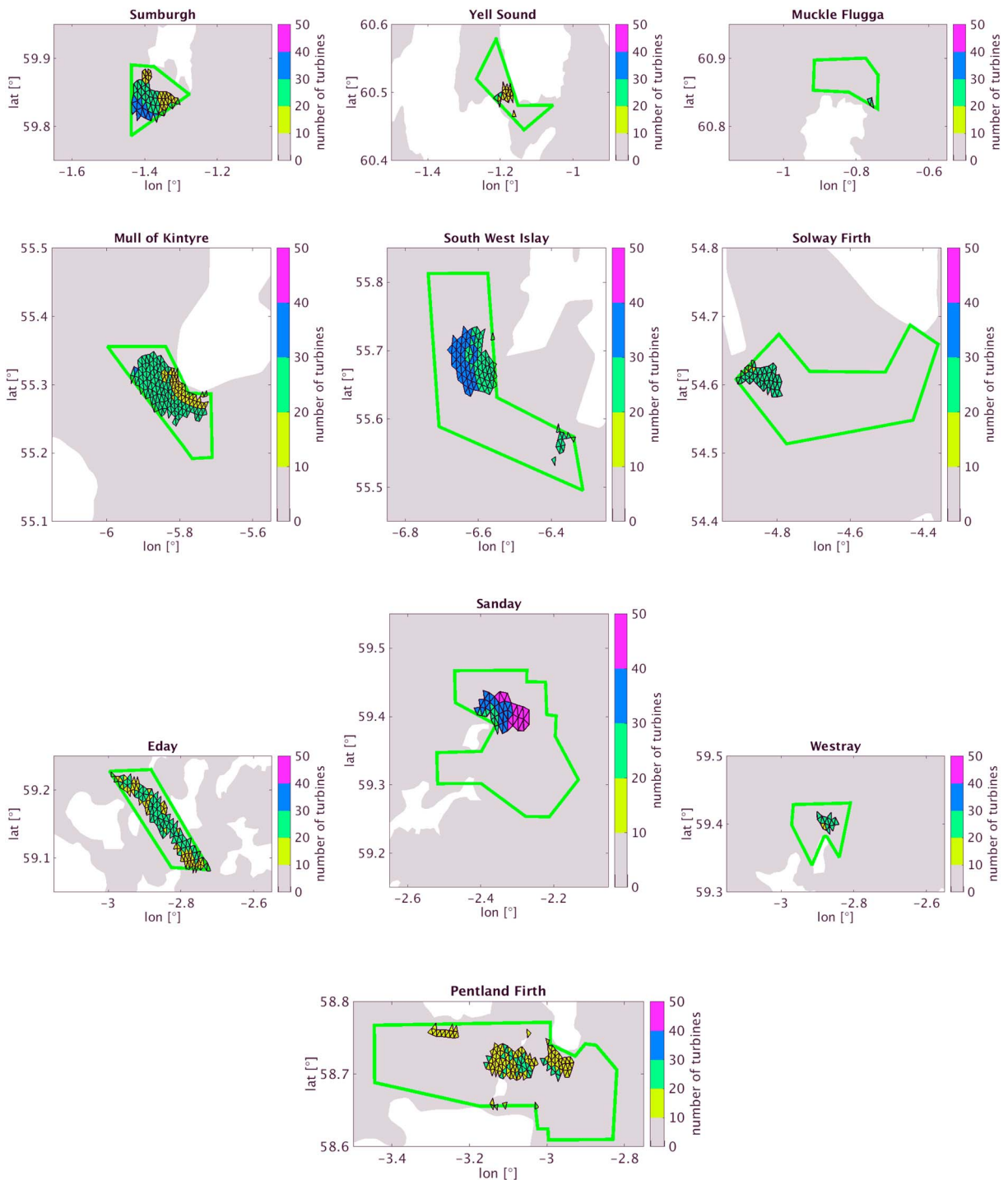


Figure 2. Number of turbines allocated in Orkney Waters (Pentland Firth, Eday, Sanday, Westray), west coast of Scotland (Mull of Kintyre, South West Islay, Solway Firth), and Shetland Islands (Sumburgh, Yell Sound, Muckle Flugga) arrays. Black contoured elements are those occupied by tidal turbines. Green lines indicate the entire areas identified for exploitation.

locations, such as Shetland Islands, we assumed turbines with a minimum rated capacity of 0.3 MW (rated speed 1.25 m/s), while for Solway Firth and South West Islay we hypothesized to use turbines with a rated capacity which can reach at lowest 0.5 MW (rated speed 1.5 m/s); for more energetic locations, such as the Mull of Kintyre and Orkney Waters, we assumed 0.7 MW (rated speed 1.75 m/s). For the Pentland Firth, the limits imposed were the same as those used by De Dominicis et al. (2017). They are a more stringent constraint than

Table 1

For Each of the 10 Tidal Plan Options: Total Number of Turbines, N_T , Average and Maximum Instantaneous Available Power, P_{AVG} and P_{MAX} , Average Power Per Turbine and Maximum Power Per Turbine, P_{AVG-T} and P_{MAX-T} and Peak Power Time Lag

Location	N_T	P_{AVG} [GW]	P_{MAX} [GW]	P_{AVG-T} [MW]	P_{MAX-T} [MW]	Time lag [hr]
Pentland Firth	2784	1.64	4.16	0.59	1.49	
Eday	2853	0.45	2.04	0.16	0.71	-0.2
Sanday	1935	0.29	1.58	0.15	0.82	+0.3
Westray	325	0.06	0.32	0.18	1.00	-0.9
Mull of Kintyre	4290	0.67	3.40	0.16	0.79	-0.6
South West Islay	3651	0.32	1.74	0.09	0.48	-0.6
Solway Firth	1379	0.13	0.79	0.09	0.57	-0.3
Sumburgh	1758	0.08	0.67	0.04	0.38	+0.3
Yell Sound	292	0.02	0.10	0.08	0.35	-0.9
Muckle Flugga	43	0.003	0.03	0.06	0.60	0

Note. Estimates are from a 30-day Scottish Shelf Model run forced by tides only with tidal stream energy extraction feedbacks included.

for the other areas, assuming that the turbine has a rated speed of 2.5 m/s, that is, rated capacity of 2 MW, and with a capacity factor limit increased to 40%. The Pentland Firth area of search has been limited to the three main channels and to the PFOW Round One Development Sites, which are the sites for commercial renewable energy development with lease agreement granted by the Crown Estate in 2010 (The Crown Estate, 2013).

The large-scale arrays have been implemented in the SSM using the momentum sink approach, in which a momentum sink term represents the loss of momentum due to tidal energy extraction. The effect of energy extraction on the fluid is simulated by implementing an additional retarding force equal and opposite to the thrust in the momentum equations. According to Newton's third law of motion, the retarding, or drag, force exerted on the flow by a turbine is equal and opposite to the thrust, \mathbf{F}_T , exerted by the flow on the turbine.

$$\mathbf{F}_T = \frac{1}{2} \rho A C_T(i, t) |\mathbf{u}| \mathbf{u} \quad (3)$$

where C_T is the thrust coefficient, A is the area swept by the turbine, and \mathbf{u} is the flow velocity. When the drag force is included in the 3-D momentum equations, we consider the number of turbines in each model element and the vertical discretization of a turbine between multiple model layers. A full description of the momentum sink approach in FVCOM can be found in Yang et al. (2013) and O'Hara Murray and Gallego (2017). The turbine thrust coefficient can either be considered constant or more realistically varied as a function of the flow speed in order to reproduce the turbine operation, which is characterized by cut-in, cut-out, and rated speed. In the present study, following De Dominicis et al. (2017), a variable thrust coefficient has been calculated using the generic (i.e., not for a specific turbine design) thrust coefficient curve constructed in Baston et al. (2015).

Since the turbines are subgrid scale objects, a number of turbines is then allocated to all model elements that are within the areas of search, with a capacity factor >35% and a depth >27.5 m. The number of turbines assigned to each model element is then the maximum number of turbines that can be allocated, considering the size of the element and the spacing limits between turbines. As shown in Figure 2 the number of turbines assigned to each model element is usually in the range 10–40. The total number allocated in Scottish Waters is $\approx 19,000$: the number of turbines assigned to each location is presented in Table 1.

2.2. Present Climate Runs

For the present day, the SSM was forced with climatologically averaged conditions for the period 1990–2014, including atmospheric forcing, temperature and salinity at the open boundary, and fresh water input from rivers along the coastline. This choice allows us to study the seasonal variability, but to ignore the interannual variability. The choice of a time-slice of 25 years as the averaging period was determined by the need to sample sufficient natural variability to be able to average out the interannual variability, while keeping the statistics within the time slice approximately stationary.

The climatological atmospheric forcing was built from a monthly 1990–2014 data set derived from ERA-Interim data (Dee et al., 2011; ERA-Interim, <https://www.ecmwf.int/en/forecasts/datasets/archive-datasets/reanalysis-datasets/era-interim>) data comprising mean sea level pressure, precipitation, evaporation, relative humidity, temperature, thermal/solar radiations, and wind (for wind, 6-hourly data were used to construct a monthly mean wind stress, which was then converted back into an equivalent wind field). Ocean boundaries have been constructed using the monthly 1990–2014 data of temperature, salinity, currents, and sea elevation provided by the Atlantic Margin Model 7 km (AMM7, O'Dea et al., 2012; Edwards et al., 2012) simulation. AMM7 is a NEMO model (Madec & the NEMO team, 2016) implementation for the NW European continental shelf. The specific run used for SSM ocean boundaries was forced by the ERA-Interim reanalysis, thus being consistent with the atmospheric forcing chosen for the SSM model run. Hourly water elevation and tidal currents were added to the climatological currents and water elevation (a representative average tidal year was selected as a climatological average for tides). Tidal currents and water elevations along the open boundary were obtained from TPXO7.2, a global model of ocean tides based on the Oregon State University tidal inversion of TOPEX/POSEIDON and Jason altimeter data (Egbert & Erofeeva, 2002). Current velocities (residual and tidal), temperature, salinity, and water elevation, after being spatially interpolated, were prescribed at all the nodes and elements of the FVCOM model boundary with a temporal resolution of 1 hr. The river runoff volume flux climatology were obtained from the Centre for Ecology and Hydrology (CEH) Grid-to-Grid (G2G) model (Bell et al., 2007, 2009; Cole & Moore, 2009), covering the period from 1962 to 2011 and including 577 rivers in Scottish Waters.

A full set of observed water level and current meter tidal analyses over the NW European Shelf and into deep water just off the shelf were used to validate the model: for tidal elevation amplitude the root-mean-square error is 0.3 m and the bias is -0.07 m, while for tidal currents the root-mean-square error is 0.1 m/s and bias is 0.02 m/s. The present climatological conditions for sea surface temperature and salinity reproduced by the SSM have been compared with the World Ocean Atlas (Boyer et al., 2013) regional climatology (see supporting information). Furthermore, the model has been also run for a specific period of time to further validate water levels, currents and temperature, and salinity against observed data (full model validation is presented in Wolf et al., 2016).

2.3. Future Climate Runs

Future climate is partly determined by the magnitude of anthropogenic emission of GHGs, aerosols, and other natural and man-made forcings. The climate system is shaped by the Earth's response to those external forcings, along with internal variability inherent in the climate system. The Representative Concentration Pathways (RCPs) describe four different 21st century pathways of GHG emissions and atmospheric concentrations, air pollutant emissions, and land use (Stocker et al., 2013) and are the basis for climate model projections. The RCPs include a stringent mitigation scenario (RCP2.6), two intermediate scenarios (RCP4.5 and RCP6.0), and one scenario with very high GHG emissions (RCP8.5; Stocker et al., 2013), termed the *business as usual* or *worst case* scenario. Different climate models provide alternative representations of the Earth's response to those forcings and of natural climate variability. For the last IPCC report, a standard set of coordinated climate model experiments were intercompared in the framework of the Coupled Model Intercomparison Project (CMIP5, <https://pcmdi.llnl.gov/mips/cmip5/>; Taylor et al., 2012). There is then a range of plausible projections for future climate that arise from the future emissions uncertainty and from the model uncertainty. One single projection (one single model and one future emission scenario) was chosen to force the SSM model: the HadGEM2-ES forced by the RCP8.5 scenario. HadGEM2-ES (The HadGEM2 Development Team et al., 2011) is a coupled Earth System Model that has been used by the Met Office Hadley Centre for the CMIP5 simulations. HadGEM2 is a configuration of the Met Office Unified Model (UM) developed from UM version 6.6. HadGEM2-ES was the first Met Office Hadley Centre model to include Earth system components as standard. The HadGEM2-ES climate model includes an atmospheric model at N96 and L38 horizontal and vertical resolution, and an ocean model with a 1° horizontal resolution (increasing to $1/3^\circ$ at the equator) and 40 vertical levels. Earth system components included are the terrestrial and ocean carbon cycle and tropospheric chemistry. This model is one of the top-performing climate models for the North Atlantic, having small biases in wintertime position and median latitude of storms, consistent with reanalysis data (Zappa et al., 2013).

For a given choice of forcing data, a straightforward approach is the direct use of the climate model data as ocean boundary and atmospheric forcing data for the present-day run and the future climate change scenario. The climate change signal is then the difference between both model run realizations. The problem with this approach is that the climate model output shows regional- and parameter-dependent biases, for

both atmospheric and ocean components. Such biases will have a significant impact on processes such as stratification and upwelling. Where these are nonlinearly dependent on the forcing variables, the biases will not cancel when the climate change signal is calculated. An alternative climate impact assessment method is the *delta-change* approach. In this method, the present-day climate forcing is provided by a present-day reference forcing, derived from the atmospheric ERA-Interim reanalysis alongside appropriate oceanic conditions (AMM7-NEMO run also forced with ERA-Interim reanalysis). This approach removes the influence of biases from the climate model forcings and preserves the mean climate change signal, which is the most robust part of the signal from climate models. The climate change forcing is then derived by perturbing the reference forcing with a multiplicative [equations (4) and (5)] or an additive spatially varying correction [equations (6) and (7)], which is a function of the future climate change forcing in relation to its present-day control:

$$\phi_f = \phi_{\text{REF}} F_M \quad (4)$$

$$F_M = \phi_{\text{RCP8.5}} / \phi_{\text{CNTRL}} \quad (5)$$

$$\phi_f = \phi_{\text{REF}} + F_A \quad (6)$$

$$F_A = \phi_{\text{RCP8.5}} - \phi_{\text{CNTRL}} \quad (7)$$

where ϕ_f is any atmospheric or oceanic model variable and F_M and F_A are the multiplication and additive corrections, respectively; f indicates the perturbed variable; REF is the reanalysis reference: 1990–2014 ERA-Interim (atmospheric forcing) and 1990–2014 AMM7-NEMO forced by ERA-Interim (ocean boundaries); CNTRL is the climate model control period: 1990–2014 HadGEM2-ES (atmospheric forcing and ocean boundaries); RCP8.5 is the climate model future scenario period: 2038–2062 (i.e., centered on 2050) HadGEM2-ES (atmospheric forcing and ocean boundaries). The river freshwater discharges were not perturbed, due to lack of information about future precipitation over Scottish catchments.

An additive correction was used for atmosphere and ocean temperature, wind and ocean current velocity component, and sea surface height (SSH). It was disregarded for the rest of the variables owing to problems with negative values of variables that are always defined positive. Since the interannual variability of the future and control simulations are not related (in time), the fields must be appropriately time averaged before calculating the perturbation to the reference simulation. We used the climatological monthly values, so preserving the seasonal cycle. HadGEM2-ES and ERA-Interim are on different grids and thus required a further interpolation step (only using sea points) before applying the delta-change approach. Additionally, the SSH correction required an ad hoc procedure. In state-of-the-art global ocean models, such as HadGEM2-ES, SSH is an anomaly with respect to the globally averaged SSH, which can have an unphysical trend in time. Global ocean models typically use the Boussinesq approximation and so conserve volume but not mass (Griffies & Greatbatch, 2012), and steric effects are calculated as a diagnostic. Thus, the additive correction for SSH has been corrected to eliminate the globally average mean sea level trend and to add the globally averaged steric sea level change (Jackson & Jevrejeva, 2016). This procedure allows the sea level rise, as predicted by the RCP8.5 scenario, to be imposed along the model domain boundary.

3. Results

3.1. Available Tidal Power Resource in Scottish Waters

The power that can be generated is dependent on the vertical cross-sectional area occupied by tidal stream turbines and is the work done by the thrust force per unit of time:

$$P(i, t) = \frac{1}{2} \rho A N(i) C_T(i, t) \overline{|\mathbf{u}(i, t)|}_T^3 \quad (8)$$

where $\overline{|\mathbf{u}(i, t)|}_T = \sum_{k=1}^{k=n} K_\sigma(i, k) |\mathbf{u}(i, k, t)|$ is the weighted average of the current speed over the diameter of the tidal turbine. It can therefore be considered to be the maximum available power for electricity generation at any instant in time.

Figure 3 shows the power provided by each location calculated from a 30-day SSM run forced by eight tidal constituents. The power calculation included the feedbacks of tidal energy extraction on the flow and assumed a variable thrust coefficient, giving us an estimate of the so-called practical resource. The specific

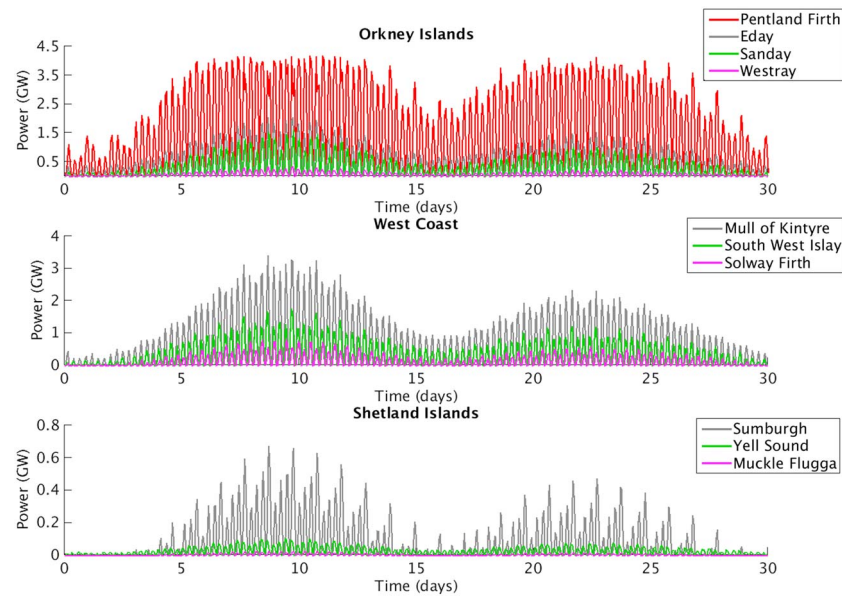


Figure 3. Power resource from a Scottish Shelf Model run forced by eight tidal constituents (M_2 , S_2 , N_2 , K_2 , K_1 , O_1 , P_1 , and Q_1) including the feedbacks of tidal stream energy extraction on the flow and using a variable thrust coefficient: Pentland Firth and Orkney Waters (top panel); west coast of Scotland (middle panel); Shetland Islands (bottom panel).

geometry of the North Sea basin implies a tidal amplification in the semidiurnal spectral range (Sündermann & Pohlmann, 2011). As a tidal energy device will generate electricity during the flood and ebb phases of the tidal cycle, peak power is available every 6 hr. The superposition of the semidiurnal principal lunar and solar tides ($M_2 + S_2$), which are in phase every ≈ 14.75 days, causes a significant spring (in-phase) and neap (out-of-phase) rhythm in the power availability. Figure 3 (top panel) shows the practical resource available from the arrays located in Orkney Waters. The temporal average power available from the Pentland Firth is 1.64 GW, in agreement with what was obtained when running the model with only the Pentland Firth array included (1.63 GW, De Dominicis et al., 2017). However, there is an increase of 0.01 GW, which is due to the combined operation of the other tidal arrays.

All the other Orkney Islands sites (Eday, Sanday, and Westray, Figure 1) can potentially provide similar power to each other. Indeed, the average per turbine is similar in the three locations, with Westray being slightly more energetic, showing a maximum power per turbine of 1 MW (see Table 1). The difference in the total amount of power provided is mainly due to the number of turbines virtually deployed in the model (Figure 2), that were constrained by depth and capacity factor limits. The Eday array scenario can produce the most power, with an average of 0.45 GW and a maximum of 2.04 GW. However, it must be noted that to achieve $\approx 30\%$ of the average practical resource available from the Pentland Firth (and half of the maximum) requires roughly the same number of turbines as deployed in the Pentland Firth (see Table 1).

Looking to the west coast of Scotland, South West Islay, and the Solway Firth (Figure 1) show equal average power per turbine (see Table 1), with the South West Islay array providing more power than the Solway Firth (Figure 3, middle panel), due to the larger number of turbines deployed (see Table 1). The Mull of Kintyre site is as energetic as the Orkney Waters locations (Eday, Sanday, and Westray), in terms of average and maximum power per turbine (see Table 1). However, given the wider area considered available for exploitation (Figure 2), a larger number of turbines were included, leading to a total average practical resource of 0.67 GW and a maximum of 3.40 GW. This appears to be the second most energetic location in Scottish Waters. It must be noted, as for Eday, that to achieve just $\approx 40\%$ of the practical resource available from the Pentland Firth, it is necessary to increase by $\approx 55\%$ the number of turbines used in the Pentland Firth. However, the Pentland Firth would require turbines with a rated power on average of 1.5 MW (see Table 1), while turbines rated at 1 MW on average would be suitable for the rest of the Orkney Waters and west coast of Scotland locations.

The Shetland Islands locations (Sumburgh, Yell Sound, and Muckle Flugga, Figure 1) are less energetic, with the lowest average (Sumburgh) and maximum power (Yell Sound) per turbine (see Table 1) and a smaller area to be exploited (Figure 2). Despite the smaller number of turbines and lower extractable power, the amount

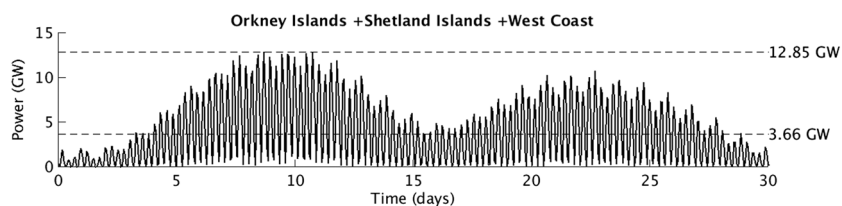


Figure 4. Aggregated power resource from all tidal arrays in Scottish Waters from a Scottish Shelf Model run forced by eight tidal constituents (M_2 , S_2 , N_2 , K_2 , K_1 , O_1 , P_1 , and Q_1) including the feedbacks of tidal stream energy extraction on the flow and using a variable thrust coefficient, with the temporal mean average and maximum values shown.

of energy available could satisfy the present Shetland Islands electricity demand (11–50 MW, Scottish Hydro Electric Power Distribution, <https://www.ssepd.co.uk/ShetlandEnergy/>). However, as Figure 3 (bottom panel) shows, the Muckle Flugga array cannot extract any power during neap tides, despite being the most energetic one during spring tides (in Shetland Waters, see maximum power per turbine in Table 1). This is due to the generic turbine design that has been considered in this work, with a cut-in speed of 1 m/s, thus not allowing any power to be generated if the flow speed is lower. For the Shetland Islands locations it would be better to deploy turbines with a lower cut-in speed, which are likely to be developed in future generations of tidal energy devices (Neill et al., 2014).

From the estimate of the practical resource available from all locations, we get an average instantaneous power of 3.66 GW. The maximum power available from all location is 12.85 GW (Figure 4), which is only slightly less than summing up the maximum power from each location (14.83 GW, see Table 1). This tells us that the peak power occurs almost at the same time in all locations, indicating minimal phase diversity among these high tidal energy sites, as also found by Neill et al. (2016). This will provide an intermittent availability of power. If we assume that a tidal energy device will generate electricity equally during the flood and ebb phases of the tidal cycle, then an optimal complementary time lag between two sites would be 3.1 hr, that is, a quarter of the tidal cycle (Neill et al., 2016). The time lag, shown in Figure 5, indicates the time of peak currents relative to the time of peak currents in the Pentland Firth, and it is calculated as the difference in the M_2 phase. It is shown that the time lags for peak currents between all the tidal arrays locations and the Pentland Firth are always within ± 1 hr, as reported in Table 1.

The practical resource available for electricity generation from each of the 10 tidal plan options has been further calculated from a 1-year fully forced SSM run with present and future climate conditions, as it is suggested by Robins et al. (2015) that even preliminary resource assessments should be based on annual average power density. We found that including the wind- and buoyancy-driven currents adds 0.01–0.03 GW to the temporal average instantaneous power available in the Pentland Firth, Sanday, Mull of Kintyre, South West Islay, and Solway Firth. The average instantaneous power available at the other locations does not increase (see Table 2). The total average power available for electricity generation is 3.78 GW. The maximum power resource is usually 0.20–0.25 GW larger than the tide-only estimation in Eday, Sanday, South West Islay, and Solway Firth (see Table 2). The maximum power does not change for the Pentland Firth, while the Mull of Kintyre location shows a peak 0.76 GW larger than the tide-only estimation (see Table 2), which might be connected to strong wind events during the year. As expected tides are thus confirmed to be the most important available contribution to the energy available from currents in these highly energetic tidal locations, with spring peak power resources that can be further enhanced if in conjunction with strong wind events.

For future climate conditions we observed that the average instantaneous practical resource either stays the same as the present day or increases by up to 0.01 GW, with peak power showing about the same values as the present climate conditions (see Table 2). Climate change will not then alter the resource estimate, which will show minimal increases in some locations and a future total average practical resource of 3.82 GW.

3.2. Impacts of Climate Change and Tidal Energy Extraction on Hydrodynamics

3.2.1. Tidal Dynamics

The ocean response to tidal stream energy extraction was first analyzed at the temporal scale of a spring-neap tidal cycle, examining changes in tidal dynamics. The main Atlantic semidiurnal M_2 Kelvin wave travels from south to north. Energy is transmitted across the shelf edge into the Celtic Sea between France and southern Ireland (Robinson, 1979). The tidal wave then progresses northward, taking 5 hr to travel from the Celtic Sea

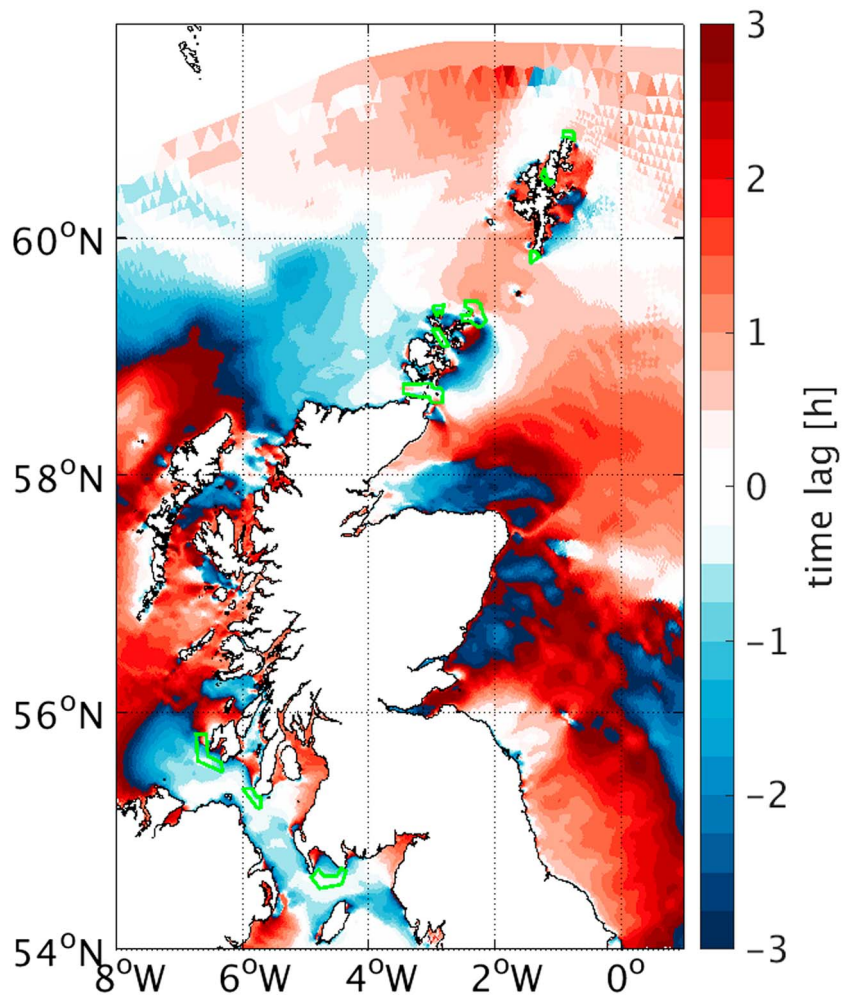


Figure 5. Time lag indicates the time of peak currents relative to the timing of peak currents in the Pentland Firth, green lines indicate areas identified for tidal energy exploitation.

to the north of Scotland, and it is partly diffracted around the north of Scotland, where it turns east, travels southward along the east coast of Scotland into the North Sea (Pugh, 1996), and moves counterclockwise as a Kelvin wave through the entire basin. Far-field effects on tidal elevation show increases upstream of the tidal farms locations (considering the direction of propagation of the tidal wave), while a decrease is observed downstream, along the UK east coast and also in the Irish Sea. A meaningful measure of change, when thinking about coastal management, is the change in the mean spring tidal range, indicating the mean tidal range during spring high and low water and thus taking into account also the influence of the S_2 tidal constituent (mean spring tidal range is defined as twice the sum of the M_2 and S_2 amplitudes). The decrease in mean spring tidal range is up to 6 cm (Figure 6c) along the whole east coast of the UK, and it is caused by the energy dissipation of the incoming Atlantic wave traveling through the tidal stream turbines in the Pentland Firth. There are also far-field changes in the tidal elevation of this magnitude upstream of the Pentland Firth, but covering a much smaller area (Figure 6c).

In the Irish Sea, the extra energy dissipation along the west coast of Scotland interacts with two Kelvin-type waves, one that progresses from the southwest through St. George's Channel and a second one that is transmitted south through the North Channel (Robinson, 1979). This generates one area of tidal range decrease in the middle of the Irish Sea and two areas of increase upstream of the north and south entrances, leading up to 6 cm increase in tidal range in the St. George's Channel (Figure 6c). As shown in Figure 6d the above mentioned changes are within $\pm 1\%$ – 2% , unless close to the amphidromes, where a small change in the amphidrome locations results in a large percentage change in tidal elevation. These changes to tidal elevation

Table 2
Average Power Per Turbine and Maximum Power for the 10 Tidal Plan Options From 1 Year Fully Forced Run With Present, P_{AVG}^{PRE} and P_{MAX}^{PRE} , and Future, P_{AVG}^{FUT} and P_{MAX}^{FUT} , Climatic Conditions

Location	P_{AVG}^{PRE} [GW]	P_{MAX}^{PRE} [GW]	P_{AVG}^{FUT} [GW]	P_{MAX}^{FUT} [GW]
Pentland Firth	1.67	4.19	1.68	4.19
Eday	0.45	2.25	0.46	2.30
Sanday	0.31	1.78	0.32	1.80
Westray	0.06	0.37	0.06	0.37
Mull of Kintyre	0.70	4.16	0.70	4.17
South West Islay	0.34	2.01	0.34	2.00
Solway Firth	0.14	1.00	0.14	1.02
Sumburgh	0.08	0.71	0.09	0.75
Yell Sound	0.02	0.11	0.03	0.12
Muckle Flugga	0.003	0.03	0.003	0.03

Note. Tidal stream energy extraction feedbacks on the flow were included.

due to tidal turbines were found to be broadly the same under the future climate hydrodynamic conditions (future baseline is in Figure 6b, differences are not shown).

Many modeling studies (Idier et al., 2017; Pelling et al., 2013; Pickering et al., 2012; Ward et al., 2012) have investigated the effect of sea level rise (SLR) on tides, and it has been suggested that even moderate SLR can have impact on the tides on the European Shelf. However, there are discrepancies between the predicted changes, mainly due to the different scenarios analyzed, spatially uniform or nonuniform SLR ranging from 0.5 m to 10 m and with no inundation (fixed coastline) or change in coastal geomorphology (allowing coastline recession) conditions. The latter has been found to be relevant only for sea level increase >1 m (Pickering et al., 2017). Our results account for a spatially nonuniform SLR, as we imposed the globally averaged steric change in sea level, as predicted by the RCP8.5 scenario, only along the model domain boundary, leading to an ≈ 15 –30 cm nonuniform SLR by 2050 in the interior of the model domain. Figure 6e shows the change in mean spring tidal range due to climate change. There is a spatial mixture of increases and decreases in mean tidal range. There are decreases in the northwest of Scotland, the western English Channel, the Shetland Islands, and north of the Southern Bight (decrease is <1 cm and <1% for the SLR scenario analyzed in this paper, very light blue in Figures 6e and 6f). The increases mainly occur in the North Sea, the eastern English Channel, the central and the southernmost Irish Sea up to the French Atlantic coast. Figure 6f shows percentage changes that exceed 5% only in the vicinity of the North Sea amphidromic points. Idier et al. (2017) analyzed a similar scenario (nonuniform, ≈ 50 cm by 2100) and found the same high-tide level pattern of changes (absolute changes are different due to different scenarios and here we are showing mean spring tidal range differences rather than high-tide level).

Comparing tidal stream energy extraction and climate change, we found that both can have an impact on tidal elevation of the order of a few centimeters. These changes broadly occur in similar geographic areas and can have the opposite effect on sea level height. Indeed, summing up the effects of tidal energy extraction and climate change (Figures 6g and 6h), the far-field decrease in the mean spring tidal range along the whole east coast of the UK, generated by the turbines' action, can possibly counteract the increase due to climate change along the same coastline. The same can be said for the Central Irish Sea. However, it should be noted that in the near-field of the tidal farms (not shown in this paper) the increase in tidal range can be the dominant effect (De Dominicis et al., 2017). The increase in tidal range on the western Scottish coast due to tidal stream energy extraction can be eventually offset by the decrease due to climate change (Figures 6g and 6h). On the other hand, the southernmost part of the Irish Sea and the Dutch coast are exposed to an increase in tidal range by both tidal stream energy extraction and climate change (Figures 6g and 6h).

Tidal currents may reach a speed of the order of several meters per second (Figure 7a) and dominate any other flow, especially as they move the entire water column. Tidal currents give rise to strong mixing of water masses, preventing thermohaline stratification in the shallow southern North Sea (Sündermann & Pohlmann, 2011). Extracting tidal stream energy from the ocean changes marine current patterns, which can be slowed down by the turbines' action or intensified due to flow diversion processes. Reduction of the mean spring

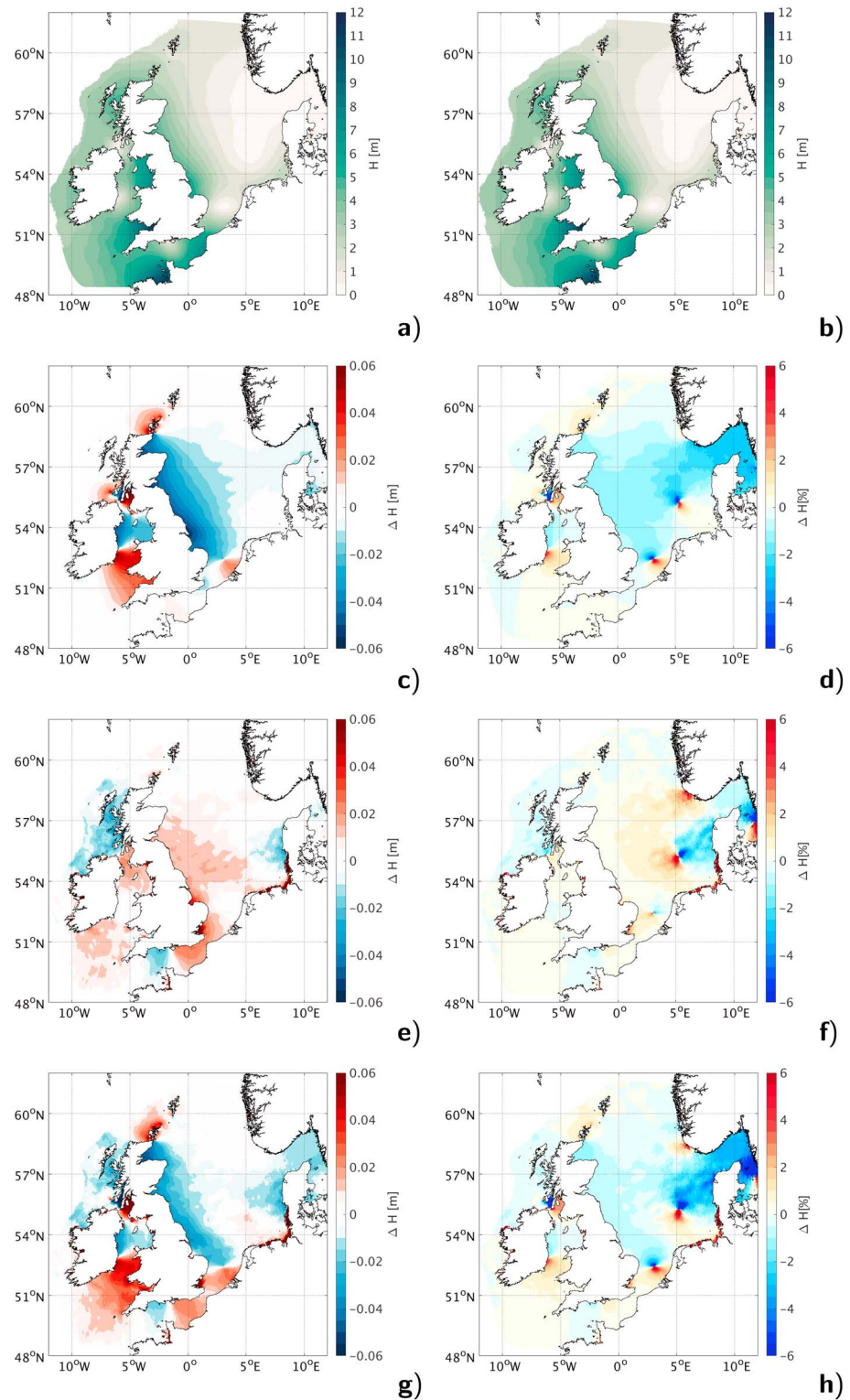


Figure 6. Spring peak tidal range during present (a) and future (b) climate conditions; change due to tidal stream energy extraction during present conditions, absolute (c) and percentage (d) difference; change due to future climate conditions, absolute (e) and percentage (f) difference; change due to tidal stream energy extraction and future climate conditions, absolute (g) and percentage (h) difference.

currents (defined as the sum of the M_2 and S_2 semimajor axis amplitudes) is of the order of few centimeters per second in the far field (Figure 7c). The pattern is generated by the interaction of different processes acting on different temporal scales: changes in ebb/flood tides, changes in tidal elevation, flow blockage, and diversion processes. The dipole velocity changes that are evident in the vicinity of the tidal arrays is due to the reduction of the ebb and flood tidal currents generated by the sink of energy in the tidal arrays. This effect is very evident both upstream and downstream of the Pentland Firth. In terms of percentage changes (Figure 7d) the decrease in velocity is larger downstream of the Pentland Firth reaching up to 8%. The same dipole ebb/flood effect is also visible in the vicinity of the tidal arrays along the west coast of Scotland: the turbines' action generates a reduction of tidal currents of the same order of magnitude as the reduction observed in the Pentland Firth, but affecting a much smaller area (Figures 7c and 7d). An increase in mean spring currents is observed in the northern Orkney Waters due the blockage of the flow into the Pentland Firth and consequent diversion (Figure 7c). Similarly, in the Irish Sea, there is an increase in mean spring currents in the vicinity of the tidal arrays that could be explained as blockage effect of the tidal arrays up to 0.02 m/s (8%) increase (Figures 7c and 7d). The increase in tidal elevation previously observed lead to changes in tidal currents too. A small reduction in current is visible along the east coast, better seen as a percentage change (Figure 7d), generated by the decrease in tidal range (Figure 6d) and a consequent water depth reduction and a friction increase. Of opposite sign is the change in tidal range at the northern and southern entrance of the Irish Sea (Figure 6d), with a consequent increase of water depth and a reduction of friction, which lead to a slight increase in tidal currents (Figure 7d). These changes to tidal currents due to tidal turbines were found to be broadly the same under the future climate hydrodynamic conditions (future baseline is in Figure 7b, difference are not shown).

There are no studies available about the change to tidal currents in the North Sea due to SLR. We found that changes in SLR together with consequent changes in tidal amplitudes act to change the tidal currents as well. The general effect is that slightly stronger tidal currents occur with SLR: increased water depth and consequent reduced friction lead to an increase in tidal currents. Figure 7f shows an overall increase of the order of 1% across the whole domain; this is modulated by bathymetry features, showing scattered larger increases or decreases. Areas where a small decrease in tidal currents is observed are deeper areas. On top of the SLR, we have the changes in tidal amplitude due to the SLR itself. This is relevant for Germany, the southeast coast of Denmark, and the southeast English coast, which show an increase in mean spring tidal currents (Figure 7e), that is where the increase in mean spring tidal range was also observed (Figure 6e). For tidal currents, the effect of providing 3.8 GW of instantaneous power is greater than climate change: the reduction in current speed is stronger (exceeding 8%, see Figure 7d) than the changes in tidal currents due to climate change (increase of 1%, Figure 7f). Indeed, summing up the effects of tidal energy extraction and climate change, they do not overlap and interact, thus showing their combined effects as the same as their stand-alone effects (see Figures 7g and 7h).

3.2.2. Stratification

Over longer-term seasonal timescales, the ocean response to tidal stream energy extraction is affected by the different present and future climate of the NW shelf hydrodynamics. As tidal stream energy extraction can reduce tidal velocities overall, and as a consequence can decrease the energy of tidal mixing, the balance between stratification and vertical mixing processes in a tidally active and seasonally stratified sea, such as the NW European continental shelf, can be perturbed. In seasonally stratified seas, the seasonal and spatial distribution of stratification can be measured through the Potential Energy Anomaly (PEA), defined as the amount of energy required to bring about complete vertical mixing per unit of volume (Simpson & Bowers, 1981). PEA is the potential energy (per unit of depth) required to fully mix the water column: where PEA is equal to zero, there is a fully mixed water column, and, for convenience, it is defined to be positive for stable stratification. Shelf waters are well mixed during winter, while during spring-summer the water column stratification onset is caused by decreased wind stress and freshwater inputs and increased summer-time heat-flux (Holt & Umlauf, 2008). The present and future climatological year model runs have been analyzed in term of winter and summer means separately to account for the strong seasonality, characteristic of the NW European continental shelf. Throughout the article, winter and summer means refer to time averages over the 3 months of DJF (December, January, February) and JJA (June, July, August), respectively.

During present climate winter conditions (Figure 8a), the water is well mixed over the entire shelf, apart from a localized area along Norway and the Kattegat, where the fresh water discharge from the Baltic Sea establishes a year-round salinity stratification, which is greater than the seasonal summer thermal stratification (Tinker et al., 2016). Winter-stratified areas are also present along the west coast of Scotland (Firth of Clyde),

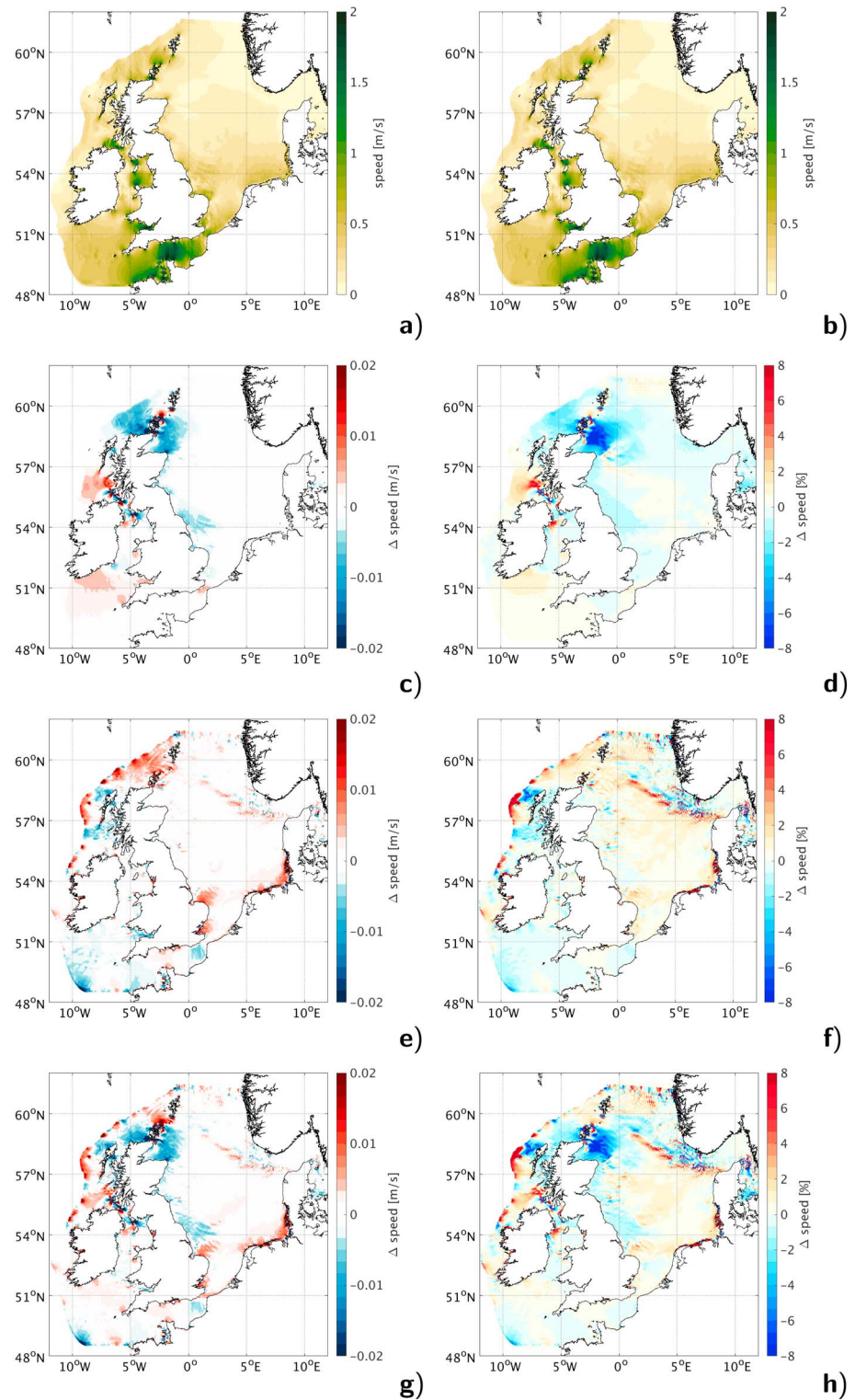


Figure 7. Spring peak tidal currents during present (a) and future (b) climate conditions; change due to tidal stream energy extraction during present conditions, absolute (c) and percentage (d) difference; change due to future climate conditions, absolute (e) and percentage (f) difference; change due to tidal stream energy extraction and future climate conditions, absolute (g) and percentage (h) difference.

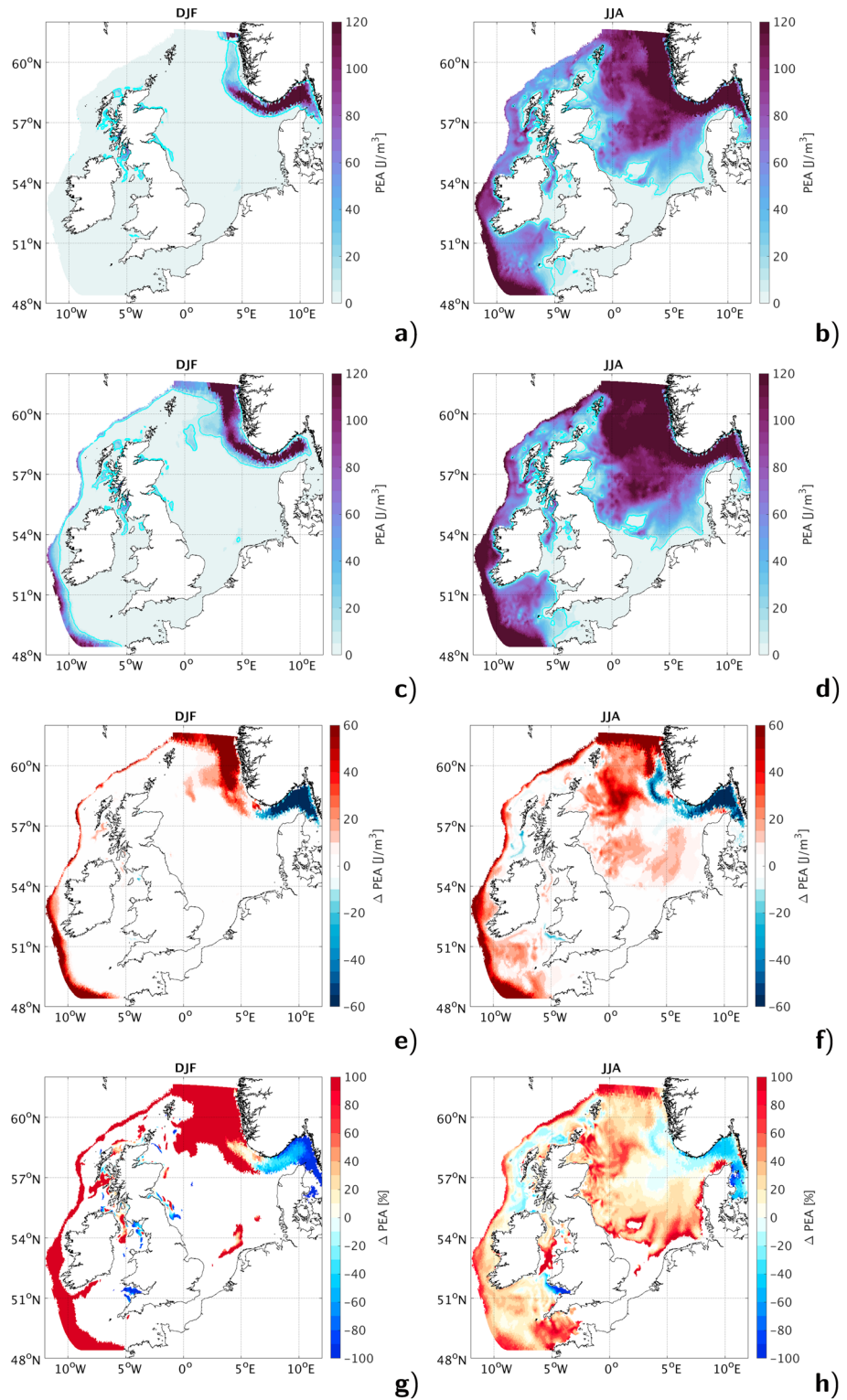


Figure 8. Potential Energy Anomaly during present climate winter = DJF (December-January-February) (a) and summer = JJA (June-July-August) (b) and during future climate winter (c) and summer (d), white line is the 10 J/m^2 contour line separating the stratified from mixed waters. Difference between the present and future climate baseline during winter (e = absolute difference, g = percentage change) and during summer (f = absolute difference, h = percentage change), masked out for clarity percentage differences associated to absolute differences less than 1 J/m^2 .

due to riverine discharges (Simpson & Rippeth, 1993). In summer the extent of mixed waters decreases, with the 10 J/m^2 contour (Figure 8b), separating stratified from mixed waters, in agreement with the position of tidal mixing fronts identified by Pingree and Griffiths (1978) and with the summer distribution of observed thermal fronts found by Miller and Christodoulou (2014).

The projected future climate in 2050, under the RCP8.5 future scenario, shows an increase in PEA on the NW European continental shelf during both winter (Figure 8c) and summer (Figure 8d). During winter the shelf waters are fully mixed with little change due to the future climate projections. However, the shelf edge and the northern Norwegian Trench show a future increase in winter stratification (Figures 8e and 8g). Those regions are influenced by the open-ocean dynamics, where stratification is mainly controlled by salinity (Holt et al., 2010; Tinker et al., 2016). Our model results predict salinity to decrease in the future both on- and off-shelf, but the freshening of the bottom layer is weaker than at the surface, leading to an increase in water column stability. This is stronger along the northern Norwegian Trench and the shelf edge (not shown, see supporting information), which are areas more influenced by the freshening of the north Atlantic. The latter is due to the future atmospheric forcing, marked by an intensifying hydrological cycle and changes in the atmospheric moisture transport (Mikolajewicz et al., 2007), which lead to an evaporation reduction over the North Atlantic predicted by the HadGEM2-ES. During summer stratification shows instead an increase $>20\%$ (Figure 8h) for most of the shelf. It is larger in the area from the northeast of Scotland toward Norway and where fronts are located in the southern North Sea and Irish Sea, where the increase can exceed 60 J/m^3 (Figure 8f). These increases are mainly dominated by the future temperature rise (Holt et al., 2010; Mathis et al., 2017; Tinker et al., 2016), as in most regions on the shelf, the temperature dominates the seasonal stratification. The SSM future projections of sea surface and bottom temperatures showed an increase during both winter and summer, with a larger surface than bottom increase during summer (not shown, see supporting information). Off the shelf, the PEA significantly increases, as already observed for future winter conditions. Changes are, instead, negligible or negative in the area of the Norwegian Trench (Figures 8f and 8h), as already found by Holt et al. (2010) and Tinker et al. (2016).

The interaction between tidal stream energy extraction and the seasonal hydrodynamic conditions for the present and future ocean state showed regionwide impacts on PEA. For present climate conditions, extracting energy to provide 3.8 GW of instantaneous power does not have any detectable influence on the predominantly well-mixed waters during winter. Indeed, changes due to tidal stream arrays operations are observable only along the west coast of Scotland and the Norwegian Trench, areas where salinity is the main driver of the winter stratification (Figure 9a). The Norwegian Trench PEA increase is negligible in terms of percentage change (Figure 9c). On the other hand, on-shelf summer stratified waters are affected by tidal stream energy extraction. Indeed, the reduction in vertical mixing due to the turbines' operations increases the strength of water stratification, mostly along the UK east coast and in the area from the northeast of Scotland toward Norway (Figure 9b). Those changes can reach an increase of 6 J/m^3 , in some limited areas (Figure 9b), corresponding to a maximum PEA increase of 20% (Figure 9d). However, the overall extent of the stratified region does not greatly change, as shown in De Dominicis et al. (2017). Thus, the enhanced biological and pelagic biodiversity hot spots, such as tidal mixing front locations, are not shifted. These are areas of enhanced concentration of nutrients and plankton, due to cross-frontal exchange processes and separate the seasonally stratified water from the permanently well-mixed waters. On the west coast, a small detected decrease in PEA (Figure 9b) can be linked to the increase in mean spring currents previously observed (Figure 7c).

Tidal stream energy extraction effects on PEA are slightly amplified by future climatic conditions. As stated before, tidal stream energy extraction noticeably affects stratified waters and since climate change stratifies waters that were mixed during present winter climate conditions, those can be then affected by turbines' action. Indeed, as shown in Figures 9e and 9g, in the future there is a detectable increase in winter PEA, generated by tidal stream energy extraction. Future summer increase in on-shelf stratification leads to an exacerbation of the impacts of the large turbine arrays in some limited areas (Figure 9f), where changes go in the same direction of those due to climate change. Those changes do not exceed 6 J/m^3 (Figure 9f) or a 20% PEA increase (Figure 9h), as was also found for present climate conditions. The summer water column stratification generated by tidal stream energy extraction during present or future climatic conditions is thus 1 order of magnitude lower than climate change effect, and over a much smaller area, driven by the temperature increase of future hydrodynamic conditions in 2050. The combined effects of climate change and tidal

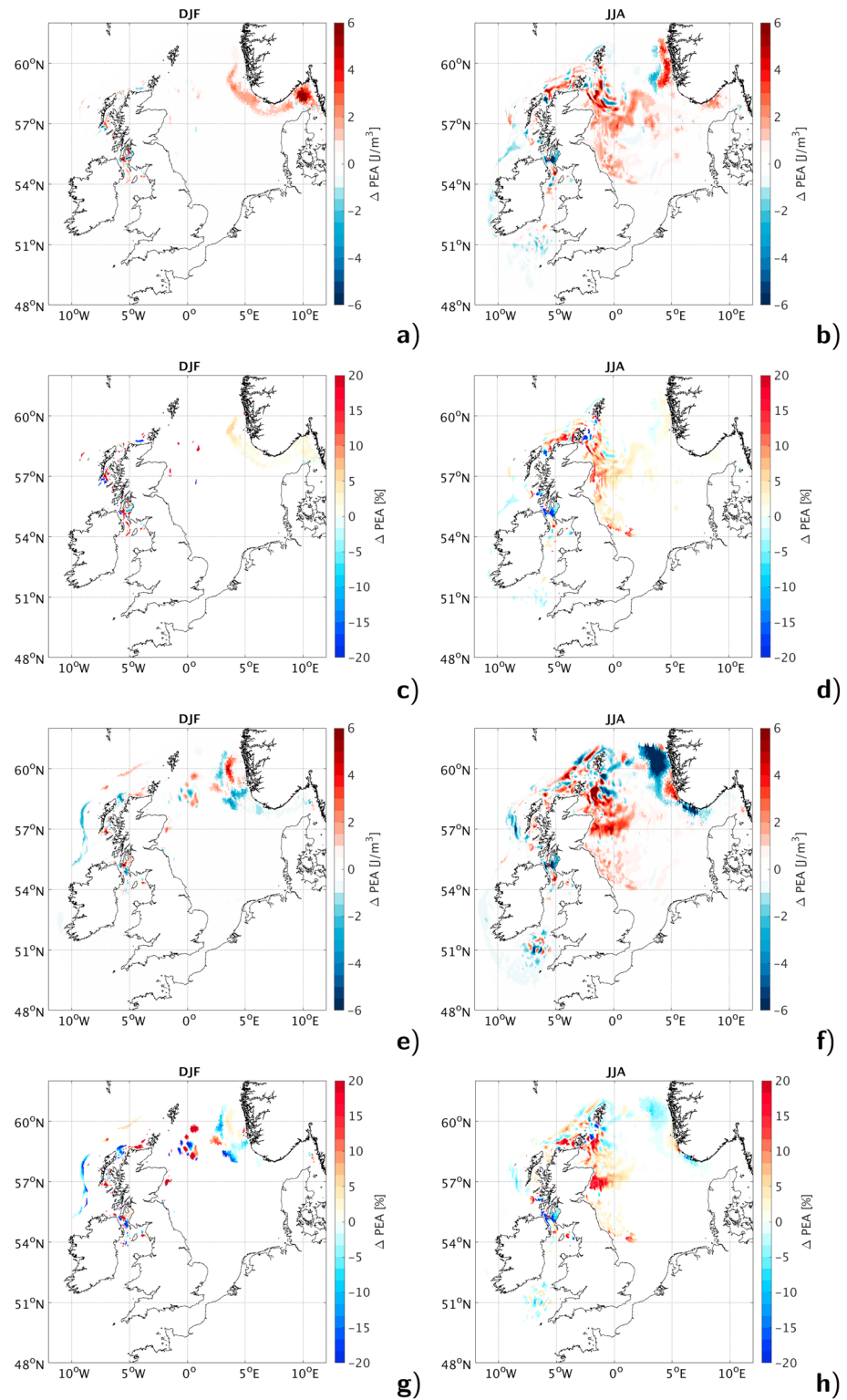


Figure 9. Change in Potential Energy Anomaly due to tidal stream energy extraction during: present winter climate (a = absolute difference, c = percentage change); present summer climate (b = absolute difference, d = percentage change), future winter climate (e = absolute difference, g = percentage change), and future summer climate (f = absolute difference, h = percentage change), masked out for clarity percentage differences associated to absolute differences less than 1 J/m^2 .

energy extraction on PEA show the same pattern (not shown) as those driven by climate change only. Indeed, being 10 times larger, those effects overcome the PEA modifications due to tidal stream energy extraction.

3.2.3. Circulation

The wind-driven circulation is the dominant permanent residual current regime that characterizes the mean current system of the North Sea. While tidal currents might be stronger, they are almost periodic with small net transport (Sündermann & Pohlmann, 2011). The thermohaline circulation is superimposed on the wind-driven one and is determined mainly by the strong seasonal variation in sea surface temperature, by the inflow of water from the Atlantic Ocean and by the freshwater supply from the continent and the Baltic Sea. The present-day climatological mean circulation reproduced by the SSM (Figures 10a and 10b) captures well the main features of the general circulation of the NW European continental shelf, a detailed description of those can be found in, for example, Turrell et al. (1992), OSPAR Commission (2000), Holt and Proctor (2008), Sündermann and Pohlmann (2011), Mathis et al. (2015), and Quante et al. (2016). The North Sea mean current system, as shown in Figures 10a and 10b, forms a cyclonic circulation pattern, which is mainly driven by the prevailing westerly winds over the NW European continental shelf (Sündermann & Pohlmann, 2011). The wind-induced circulation is particularly strong in winter when wind speeds are higher, as shown in Figure 10a compared to Figure 10b. On the western side of the model domain, the density-driven currents provide a continuous route from the French coastal region via the Celtic shelf and west of Ireland to the Scottish Shelf (Hill et al., 2008; Holt & Proctor, 2008) and are stronger during summer (Figure 10b). To ease the analysis of the results, the modeled three-dimensional current fields have been condensed to two-dimensional horizontal fields by depth-averaging, thus including the signals of deeper layers. Depth-averaged rather than depth-integrated values help to highlight the shelf areas.

The comparison between present (Figures 10a and 10b) and future (Figures 10c and 10d) general circulation shows a weaker future cyclonic circulation in the North Sea, both in summer (Figures 10f and 10h) and winter (Figures 10e and 10g). This can be caused by changes in the wind patterns and less water exchange with the Atlantic. This change would have negative consequences for the North Sea's ecosystem, which has become adapted to a major cyclonic drift of water masses (Sündermann & Pohlmann, 2011). A reduction of the inflow of Atlantic water through the Fair-Isle Passage (between Orkney and Shetland Islands) and the Dover Strait is also visible, more pronounced during winter. A weaker Dooley Current, the northernmost recirculation cell, is caused by the reduced Fair-Isle inflow. Similar findings are described by Mathis and Pohlmann (2014) and Tinker et al. (2016). The Scottish coastal water, the Central and South North Sea water, and the Continental coastal water currents are also slightly reduced, in particular, during winter (Figures 10e and 10g). A reduction of the Skagerrak recirculation is also observed.

A strengthening of the European slope current is visible on the western side, particularly during summer (Figures 10f and 10h), while during winter, an enhancement of the Irish coastal current is detected (Figures 10e and 10g). A slight increase of the northern inflow is also indicated through the increasing current speed northeast of the Shetland Islands. However, during both seasons, a reduction of the inflow of Atlantic water along the Norwegian trench is observed (Figures 10e, 10f, 10g, and 10h), as found also by Mathis and Pohlmann (2014). The large increase in current speed shown at the northeast corner of Figures 10e, 10f, 10g, and 10h is due to a shift in position, and detaching from the coast, of the Norwegian Coastal Current, that brings freshwater into the North Sea and is the only net outflow of the North Sea water into the Atlantic. Additionally, the SSM shows an increase in a northward flow east of Shetland Islands (at $\sim 2^\circ\text{E}$ in summer, Figure 10b) and the appearance of a southward inflow close to the Norwegian coast (winter and summer, Figures 10c and 10d, respectively). Similar patterns have been shown by Mathis and Pohlmann (2014) and Tinker et al. (2016), who observed that the weakening of the Dooley current might lead to a substantial proportion of the northern inflow to reverse shortly after entering the northern North Sea, leading to an increase in the Norwegian Coastal Current or to a northwestward flow parallel to the Norwegian Coastal Current.

As shown in Figures 11a and 11b, with present climate conditions, the effects of tidal energy extraction on residual currents are observed mainly in the vicinity of the tidal turbine arrays, in the Pentland Firth, between Orkney and Shetland, and in the Irish Sea. Changes further propagate during winter in the Fair-Isle inflow region and up to the Dooley Current region during summer. Changes can lead to a decrease/increase up to 0.02 m/s, which are more intense and over a wider area during summer than in winter (Figures 11a and 11b). Those changes account for 40% of the residual water velocity in the affected region (Figures 11c and 11d). However, it must be noticed that changes in the area are both positive/negative, they can thus be explained by currents being shifted, rather than an enhancement/reduction of the Fair-Isle inflow. The climate change

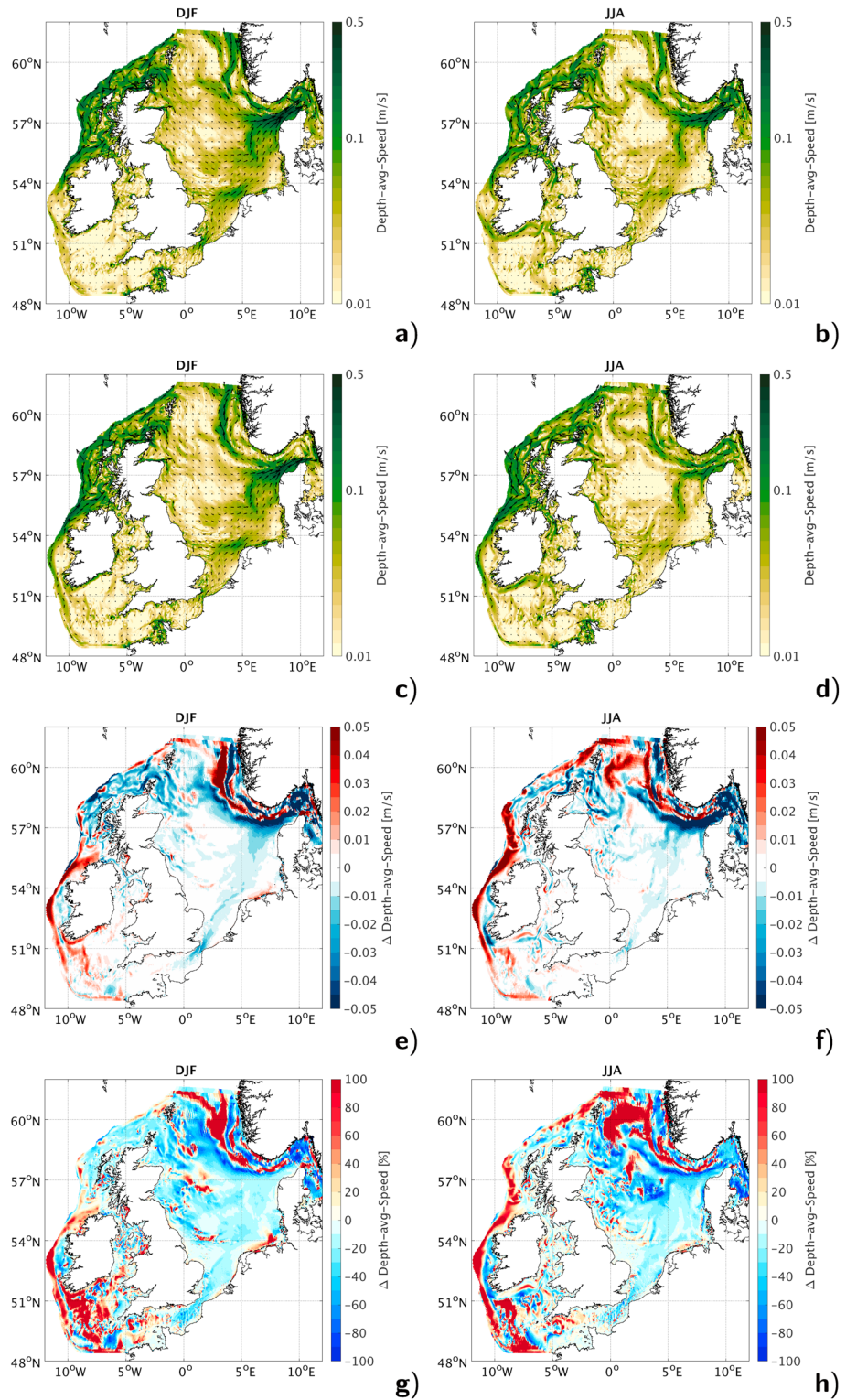


Figure 10. Depth-averaged currents during present climate winter = DJF (December-January-February) (a) and summer = JJA (June-July-August) (b) and during future climate winter (c) and summer (d). Difference between the present and future climate baseline during winter (e = absolute difference, g = percentage change) and during summer (f = absolute difference, h = percentage change).

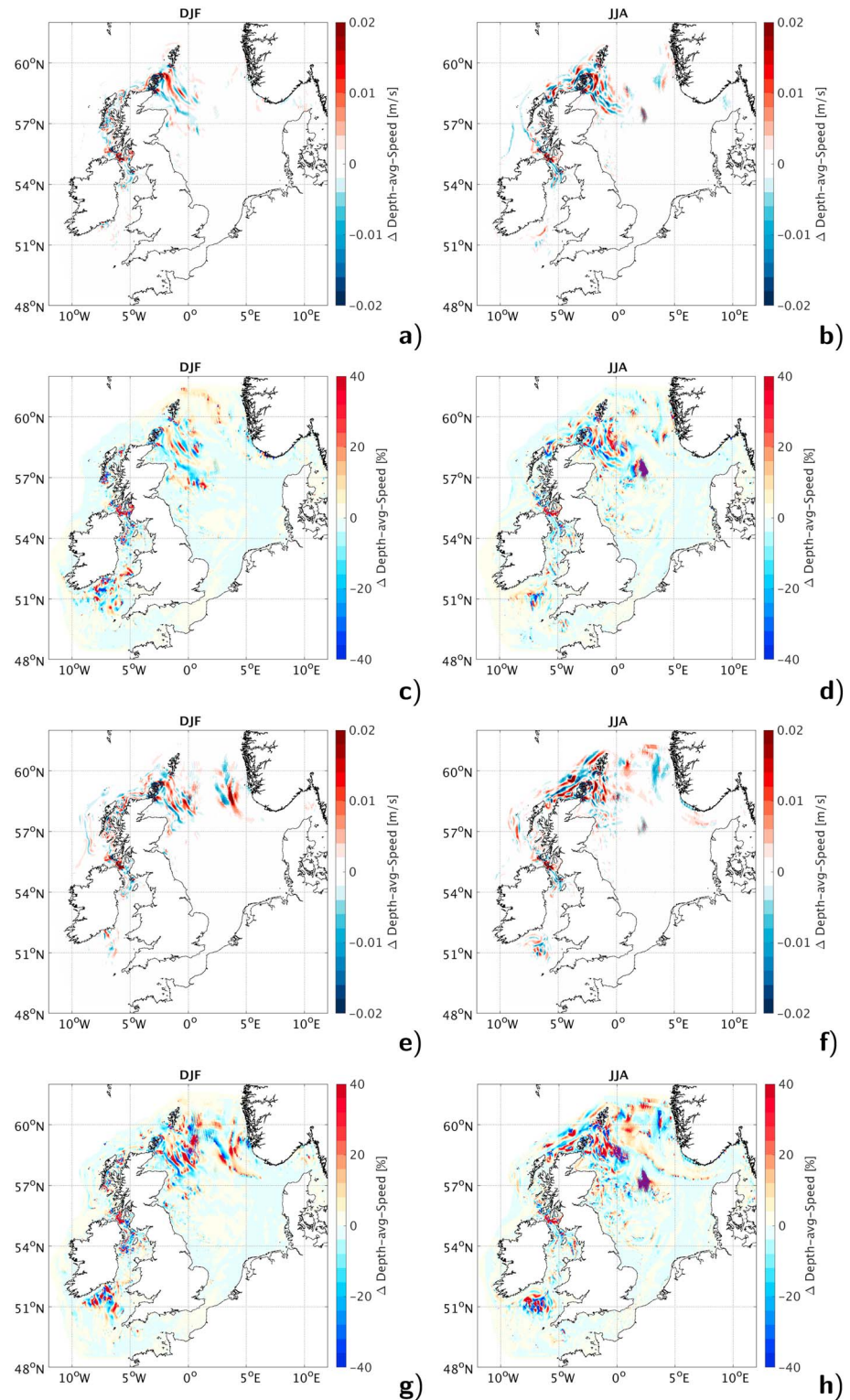


Figure 11. Change in depth-averaged currents due to tidal stream energy extraction during: present winter climate (a = absolute difference, c = percentage change); present summer climate (b = absolute difference, d = percentage change), future winter climate (e = absolute difference, g = percentage change) and future summer climate (f = absolute difference, h = percentage change).

scenario previously analyzed was showing a coherent reduction of currents speed in the Fair-Isle inflow, that could reach 0.05 m/s (Figures 10e and 10f). In the Irish Sea, a decrease/increase in residual currents is also observed, although confined to the vicinity of the tidal turbine arrays.

Future climate conditions show a pattern similar to the one observed for present climate. Currents look to be shifted, given the alternation of decrease/increase of current speed. Changes are of the same magnitude of the ones observed during present conditions. However, an exacerbation of changes given future climate conditions is observed only in the extent of the perturbed areas, being wider, in particular, during summer, extending up to the Norwegian Trench and on western side up to the shelf break (Figures 11e and 11f). Although percentage changes can exceed 40% (Figures 11g and 11h), showing pattern of propagation of the changes up to the southern entrance of the Irish Sea, absolute changes do not exceed 0.02 m/s. The impacts of extracting energy to provide 3.8 GW of instantaneous power appear to be smaller, over a restricted area and less consistent than the impacts on residual currents generated by the future climate projection considered in this work. Indeed, the effects of climate change on the residual circulation largely overcome the modifications due to tidal stream energy extraction. The combined effects of climate change and tidal energy extraction show the same pattern (not shown) as those driven by climate change only.

4. Discussion

Renewable energy is a strategy to lower CO₂ emissions and to mitigate climate change (Edenhofer et al., 2011). The global use of fossil fuels has increased, since the Industrial Revolution, to meet the energy requirements of basic human needs and productive processes. However, we have learned, while already experiencing their effect, that fossil fuels contribute significantly to the CO₂ emissions, among other environmental problems. Energy conservation and efficiency, renewable energy, nuclear energy, and carbon capture and storage are available strategies for satisfying the energy needs, while lowering GHG emissions. However, an open question is whether all of these energy options are free of any side effects. It is better to learn this before making our energy system reliant on them. The aim of this work was therefore to analyze the potential impacts of tidal energy extraction on the marine environment, as they should be considered when planning future tidal energy exploitation. We wanted to put them in the broader context of the possibly greater and global ecological threat of climate change. Extracting energy is not without its own consequences, but negative effects of climate change can be worse, as demonstrated in this work. Moreover, while marine renewable energy alleviates the climate change impacts, by reducing emissions, with a positive effect on a global scale, its side effects will be mostly on a local scale. A key result of this study is that those local effects are not only negative ones. For example, we found that tidal stream energy extraction could ameliorate the undesirable effects of rising mean sea level in some locations. This is relevant from the perspective of the development of marine renewable energy industry, that can be seen, in some occasions, as a mitigation measure for climate change, not only on a global scale, but also on a local one (e.g., coastal defence).

The value 3.8 GW is a realistic estimate of the average instantaneous power that can be provided from Scottish Waters. However, such large-scale tidal stream energy extraction is unlikely to occur in the near future, since very large numbers of devices are required. It must be noted that some power will be lost during the electricity generation process and, while the generic tidal turbine parameters used are acceptable to stakeholders (Baston et al., 2015), more or less energy could be potentially generated by using other types of devices and/or different array layouts. With the strongest currents in Scottish Waters, the Pentland Firth gives almost half of the total power (1.67 GW) and it requires fewer turbines at the same power output, but with a larger rated capacity (2 MW). The other areas would not need such large devices. Turbine design is important, for example, turbines not working below 1 m/s would not be optimal in some Shetland Islands locations. As we found in this work, they would not produce any power during neap tides and a lower cut-in speed should be developed in future generations of tidal energy devices (Neill et al., 2014). The turbines used in this study approximate to the current best technology; however, in the future the development of devices that are able to exploit deeper locations or floating turbine platforms (Zhou et al., 2017) may yield a different resource estimate. Turbines suitable for exploiting lower-energy sites can also lead to an increase of the resource available (Lewis et al., 2015; Neill et al., 2017). Furthermore, less energetic tidal sites should be considered for future developments, as they offer less challenging environments in which to operate and more tidal energy phase diversity among the different sites (Lewis et al., 2015; Neill et al., 2017). The latter is an important factor to consider when planning tidal array locations. Given the inherent intermittency of tidal power (undesirable from a grid integration perspective), it would be advisable to compensate this with tidal arrays that are lagged in phase.

The arrays considered in this work have shown instead a phase lag never exceeding 1 hr, while the optimal one would be a quarter of the tidal cycle or about 3 hr (Neill et al., 2016).

The action of very large scale tidal arrays on a seasonally stratified shelf sea was evaluated by comparing a set of ocean physical parameters describing the hydrodynamic conditions representative of present and projected future climate in 2050, provided by the SSM model simulations. This work considered only the RCP8.5 scenario, the worst case with very high GHG emissions, which gives a plausible pathway, upon which the HadGEM2-ES climate model projection (the forcing of our future climate run) is based. Although all models are built on the same physical principles, some choices and approximations are needed, which include unrefined representation of known processes and inclusion or not of some processes in the models. These choices produce differences in climate projections from different models. There is then a range in plausible projections for future climate that arise from the future emissions uncertainty and from the model uncertainty. Although HadGEM2-ES is one of the top-performing climate models of the North Atlantic, we presented only a single realization of future conditions and, also, only one possible tidal stream array layout; thus, our results should be seen as physically plausible projections, rather than a prediction. Exact numbers are not the object of this work, since we were looking for relative changes induced by two anthropogenic factors that could shape the future NW European shelf dynamics. Besides model structural uncertainties, both of the forcing of the model and of the shelf seas model, it is reassuring that our findings are broadly in agreement with previous climate change impact studies, which include SLR prediction and extreme water levels changes (Idier et al., 2017; Pelling et al., 2013; Pickering et al., 2012; Ward et al., 2012), a warming and freshening of the North Sea and consequent stratification increase and general circulation changes (Ådlandsvik, 2008; Holt et al., 2010; Mathis et al., 2017; Mathis & Pohlmann, 2014; Schrum et al., 2016; Tinker et al., 2016). However, the amplitude and exact spatial pattern of the projected changes still remain uncertain due to the difference in reference periods and emissions scenarios from the existing literature.

The inter-annual variability (natural and of the induced anthropogenic changes) cannot be assessed in this study. The delta-change method has the main advantage that it only requires one additional simulation for estimating the climate change impact, that can be estimated as the difference between the present-day SSM run forced with the reference reanalysis data and the model run with the perturbed future forcings. One of the general disadvantages of the delta-change approach is the loss of information about inter-annual variability. However, in our specific case, the SSM model for the present-day climate was forced with climatological averages and the inter-annual variability was already neglected. This choice came from computational resource limitations, which make a multi-year FVCOM simulation impractical. Essentially we asked: how would average conditions in 2038–2062 differ from those in 1990–2014, assuming the inter-annual variability remains the same?

The SSM model has been proven to be a very useful tool, since it allows us to study the effects over the entire NW European Shelf with a minimum spatial resolution (500 m to 1 km) that permits the resolution of the tidal stream energy sites (Lewis et al., 2015). However, higher resolution might allow further improvements in the representation of tidal stream turbines in the model, leading to both more accurate estimate of power and environmental effects, those include the following: (i) small scale (<1 km) interactions between turbine wakes to be reproduced; (ii) optimization techniques to be applied for the positioning and individual tuning of turbines that could potentially increase the extracted energy (Funke et al., 2014); (iii) changes in turbulence due to turbines' action for a correct reproduction of mixing behind turbines (Li et al., 2017). Additionally, a momentum sink term due to the drag of the physical structures of turbine blades, supporting poles, and foundations (Yang et al., 2013) can also be considered.

It has been shown that both climate change and the very large tidal stream arrays can introduce detectable changes to the tidal elevation, marine (tidal and residual) currents, and ocean stratification patterns. How do those changes in the physical ocean conditions translate into impacts on ecosystem habitats and animals' behavior? This is being answered by further studies looking at the possible consequences on the marine ecosystem of the effects of climate change with those of tidal stream energy extraction. The NW European continental shelf is a biologically rich region, inhabited by diverse species of all trophic levels. A complex network of interactions between biota and the physical environment characterizes the marine shelf ecosystem, where patterns in habitat use can coincide with particular oceanographic conditions: temperature, currents, frontal activity, the strength of the tidal currents, which also affect primary productivity (Cox et al., 2016; Sadykova et al., 2017). Ongoing studies are evaluating whether the predicted physical changes due to tidal

stream energy extraction and climate change will affect the availability and location of critical habitats for marine species and, as a consequence, changes in animal behaviors. This can be done by means of statistical models that use as input the results of the present work and explore the distributions of mobile predator and prey species, such as pelagic fish and seabird and marine mammal species, to calculate the degree of overlap in these species now and in future predictions.

Ongoing studies are also assessing if the reduction in tidal currents presented in this work and the consequent reduction in bed shear stress could lead to significant changes in water turbidity, as already suggested by Heath et al. (2016). On the other hand, the localized areas where an increase in currents has been detected need further investigation, in particular, where sediments could be mobilized, as done on a smaller scale by Fairley et al. (2015) and Martin-Short et al. (2015). Moreover, impacts on benthic communities is also an ongoing topic of research. However, the effect of tidal energy extraction on benthos might be negligible, since their composition is stable over an approximate 1 m/s range of velocities in high-velocity flow environments (Kregting et al., 2016), which is above the range of changes we found; an overall habitat loss might instead be predicted to occur in response to climate change.

Modifications in the extent of the stratified areas mean shifting the position of tidal mixing fronts, thus of enhanced biological and pelagic biodiversity hot spots, as well as changes in PEA that can trigger phytoplankton blooms. If a decrease in water turbidity is detected, it can in turn increase sunlight penetration and consequently lead to higher primary productivity, possibly affecting the ecosystem habitats. Since stratification and turbidity changes can have consequences on the ecosystem biogeochemistry, future work should involve the use of a biogeochemical model to properly evaluate the impacts of changes of physical factors on marine primary productivity and nutrients distribution. This would be beneficial to better link the physical changes with ecological impacts. In addition, changes in residual circulation are usually an overlooked stressor acting on marine ecosystems, but consequences are beginning to emerge (van Gennip et al., 2017). Future studies are needed to properly assess if the detected changes in residual currents, both due to climate change and tidal energy extraction, can lead to changes in transport pathways of passive tracers, affecting larval transport and dispersal, and possibly population connectivity.

5. Conclusions

This study provides a plausible projection of how the hydrodynamic conditions on the NW European continental shelf might respond to climate change and to tidal stream energy extraction. It responds to a substantial increase in the demand for evidence-based policy advice for marine climate change and offshore renewable energy. We numerically simulated changes in the physical marine environment of a shelf sea, induced by both the business as usual future climate scenario (RCP8.5) and by hypothetical very large tidal stream arrays in Scottish Waters (UK), able to provide 3.8 GW for electricity generation. This is about 10% of the UK's present average instantaneous electricity consumption (Department for Business, 2016). Tides have been confirmed to be the most important contribution to energy available from the currents. Climate change will not alter the energy resource estimate, which will show minimal increases in some locations due to increases in tidal currents driven by SLR. Such large-scale tidal stream energy extraction is realistic but unlikely to occur in the near future. It is an extreme best (worst in terms of impacts) case scenario to explore the environmental effects.

The potential effect of climate change on the ocean system have been evaluated and compared with the present and the future state of the seas modified by large-scale energy extraction. It has been shown that the very large scale tidal stream energy extraction can introduce detectable changes to the tidal range, which mainly increases upstream of the tidal farm locations (considering the direction of propagation of the tidal wave), while a decrease in the mean spring tidal range is observed downstream, along the UK east coast and also in the Irish Sea. Those effects are found not to be exacerbated by future climate conditions. Although changes are small, of the order of a few centimeters, the tidal range reduction in some cases may act to counter the predicted rise in sea level due to climate change by reducing extreme water levels.

Currents (both tidal and residual) are slowed down due to the sink of energy in the tidal arrays or speeded up due to flow diversion and blocking. While the business as usual future climate scenario can induce larger impacts in the residual current circulation than the tidal stream arrays, tidal velocities show greater changes due to tidal energy extraction. The strongest signal in tidal velocities is an overall reduction that can have consequences on a seasonal temporal scale. Indeed, the strength of summer stratification on the NW European continental shelf is found to slightly increase, due to the tidal velocities decrease and, as a consequence, tidal

mixing. A key finding is that climate change effects and tidal energy extraction both act in the same way in terms of increasing stratification due to warming and reduced mixing. However, the future increase in summer water column stratification driven by the temperature increase is 10 times larger and over a much wider area than the one generated by tidal stream energy extraction during present or future climate conditions.

The results presented in this work are the basis for other ongoing studies that evaluate the impacts of the above mentioned physical changes on animal behaviors, in particular, the distributions of mobile predator and prey species, on sediment dynamics with special attention to water turbidity, and on benthic communities.

Acknowledgments

This work is part of the EcoWatt2050 project, funded by the Engineering and Physical Sciences Research Council (EPSRC), grant reference EP-K012851-1. The work was also supported by NOC National Capability programme in Ocean Modelling. The SSM model runs produced for the EcoWatt2050 project are hosted by Marine Scotland at <https://data.marine.gov.scot/group/oceanography>. Authors acknowledge the World Climate Research Programme's Working Group on Coupled Modeling, which is responsible for the CMIP5 and the Met Office Hadley Centre for producing and making available the HadGEM2-ES model output. The data used are listed in the references.

References

- Ådlandsvik, B. (2008). Marine downscaling of a future climate scenario for the North Sea. *Tellus A*, *60*(3), 451–458.
- Baston, S., Waldman, S., & Side, J. (2015). Modelling energy extraction in tidal flows. In *TeraWatt Position Papers* (1st ed., chap 4, pp. 75–107). MASTS.
- Bedard, R., Previsic, M., Polagye, B., Hagerman, G., & Casavant, A. (2006). North America tidal in-stream energy conversion technology feasibility study (EPRI Report TP008), EPRI, Palo Alto, CA.
- Bell, V., Kay, A., Jones, R., & Moore, R. (2007). Development of a high resolution grid-based river flow model for use with regional climate model output. *Hydrology and Earth System Sciences*, *11*(1), 532–549.
- Bell, V., Kay, A., Jones, R., Moore, R., & Reynard, N. (2009). Use of soil data in a grid-based hydrological model to estimate spatial variation in changing flood risk across the UK. *Journal of Hydrology*, *377*(3), 335–350.
- Boyer, T. P., Antonov, J. I., Baranova, O. K., Coleman, C., Garcia, H. E., Grodsky, A., et al. (2013). World Ocean Database 2013. In S. Levitus & A. Mishonov (Eds.), *NOAA Atlas NESDIS 72* (209 pp.).
- Chen, C., Liu, H., & Beardsley, R. C. (2003). An unstructured grid, finite-volume, three-dimensional, primitive equations ocean model: Application to coastal ocean and estuaries. *Journal of Atmospheric and Oceanic Technology*, *20*(1), 159–186.
- Cole, S. J., & Moore, R. J. (2009). Distributed hydrological modelling using weather radar in gauged and ungauged basins. *Advances in Water Resources*, *32*(7), 1107–1120.
- Cox, S., Witt, M., Embling, C., Godley, B., Hosegood, P., Miller, P., et al. (2016). Temporal patterns in habitat use by small cetaceans at an oceanographically dynamic marine renewable energy test site in the Celtic Sea. *Deep Sea Research Part II: Topical Studies in Oceanography*, *141*, 178–190.
- De Dominicis, M., O'Hara Murray, R., & Wolf, J. (2017). Multi-scale ocean response to a large tidal stream turbine array. *Renewable Energy*, *114*, 1160–1179.
- Dee, D. P., Uppala, S. M., Simmons, A. J., Berrisford, P., Poli, P., Kobayashi, S., et al. (2011). The ERA-Interim reanalysis: Configuration and performance of the data assimilation system. *Quarterly Journal of the Royal Meteorological Society*, *137*(656), 553–597.
- Department for Business, Energy & Industrial Strategy (2016). Electricity: Chapter 5, Digest of United Kingdom Energy Statistics (DUKES). Retrieved from <https://www.gov.uk/government/statistics/electricity-chapter-5-digest-of-united-kingdom-energy-statistics-dukes>
- Edenhofer, O., Pichs-Madruga, R., Sokona, Y., Seyboth, K., Matschoss, P., Kadner, S., et al. (2011). *IPCC special report on renewable energy sources and climate change mitigation*. Cambridge, UK and New York: Cambridge University Press.
- Edwards, K., Barciela, R., & Butenschon, M. (2012). Validation of the NEMO-ERSEM operational ecosystem model for the North West European Continental Shelf. *Ocean Science*, *8*, 983–1000.
- Egbert, G. D., & Erofeeva, S. Y. (2002). Efficient inverse modeling of barotropic ocean tides. *Journal of Atmospheric and Oceanic Technology*, *19*(2), 183–204.
- European Commission (2011). *Communication from the Commission to the European Parliament, the Council, the European Economic and Social Committee of the Regions: Energy Roadmap 2050 (COM(2011) 885 final of 15 December 2011)*. Brussels: European Commission.
- Fairley, I., Masters, I., & Karunarathna, H. (2015). The cumulative impact of tidal stream turbine arrays on sediment transport in the Pentland Firth. *Renewable Energy*, *80*, 755–769.
- Funke, S. W., Farrell, P. E., & Piggott, M. (2014). Tidal turbine array optimisation using the adjoint approach. *Renewable Energy*, *63*, 658–673.
- Griffies, S. M., & Greatbatch, R. J. (2012). Physical processes that impact the evolution of global mean sea level in ocean climate models. *Ocean Modelling*, *51*, 37–72.
- Hasegawa, D., Sheng, J., Greenberg, D. A., & Thompson, K. R. (2011). Far-field effects of tidal energy extraction in the Minas Passage on tidal circulation in the Bay of Fundy and Gulf of Maine using a nested-grid coastal circulation model. *Ocean Dynamics*, *61*(11), 1845–1868.
- Heath, M., Sabatino, A., Serpetti, N., McCaig, C., & O'Hara Murray, R. (2016). Modelling the sensitivity of suspended sediment profiles to tidal current and wave conditions. *Ocean and Coastal Management*, *147*, 49–66.
- Hill, A., Brown, J., Fernand, L., Holt, J., Horsburgh, K., Proctor, R., et al. (2008). Thermohaline circulation of shallow tidal seas. *Geophysical Research Letters*, *35*, L11605. <https://doi.org/10.1029/2008GL033459>
- Holt, J., & Proctor, R. (2008). The seasonal circulation and volume transport on the Northwest European continental shelf: A fine-resolution model study. *Journal of Geophysical Research*, *113*, C06021. <https://doi.org/10.1029/2006JC004034>
- Holt, J., & Umlauf, L. (2008). Modelling the tidal mixing fronts and seasonal stratification of the Northwest European continental shelf. *Continental Shelf Research*, *28*(7), 887–903.
- Holt, J., Wakelin, S., Lowe, J., & Tinker, J. (2010). The potential impacts of climate change on the hydrography of the Northwest European continental shelf. *Progress in Oceanography*, *56*(3), 361–379.
- Holt, J., Butenschon, M., Wakelin, S., Artioli, Y., & Allen, J. (2012). Oceanic controls on the primary production of the Northwest European continental shelf: Model experiments under recent past conditions and a potential future scenario. *Biogeosciences*, *9*, 97–117.
- Idier, D., Paris, F., Le Cozannet, G., Boulahya, F., & Dumas, F. (2017). Sea-level rise impacts on the tides of the European shelf. *Continental Shelf Research*, *137*, 56–71.
- Jackson, L. P., & Jevrejeva, S. (2016). A probabilistic approach to 21st century regional sea-level projections using RCP and high-end scenarios. *Global and Planetary Change*, *146*, 179–189.
- Karsten, R., McMillan, J., Lickley, M., & Haynes, R. (2008). Assessment of tidal current energy in the Minas Passage, Bay of Fundy. *Proceedings of the Institution of Mechanical Engineers, Part A: Journal of Power and Energy*, *222*(5), 493–507.
- Kregting, L., Elsaesser, B., Kennedy, R., Smyth, D., O'Carroll, J., & Savidge, G. (2016). Do changes in current flow as a result of arrays of tidal turbines have an effect on benthic communities? *PloS one*, *11*(8), e0161279.

- Lewis, M., Neill, S., Robins, P., & Hashemi, M. (2015). Resource assessment for future generations of tidal-stream energy arrays. *Energy*, *83*, 403–415.
- Li, X., Li, M., McLelland, S. J., Jordan, L.-B., Simmons, S. M., Amoudry, L. O., et al. (2017). Modelling tidal stream turbines in a three-dimensional wave-current fully coupled oceanographic model. *Renewable Energy*, *114*, 297–307.
- Madec, G., & the NEMO team (2016). *NEMO ocean engine—version 3.6 stable. Note du pole de modélisation*. France: No 27, Institut Pierre-Simon Laplace (IPSL).
- Martin-Short, R., Hill, J., Kramer, S., Avdis, A., Allison, P., & Piggott, M. (2015). Tidal resource extraction in the Pentland Firth, UK: Potential impacts on flow regime and sediment transport in the Inner Sound of Stroma. *Renewable Energy*, *76*, 596–607.
- Mathis, M., & Pohlmann, T. (2014). Projection of physical conditions in the North Sea for the 21st century. *Climate Research*, *61*(1), 1–17.
- Mathis, M., Elizalde, A., Mikolajewicz, U., & Pohlmann, T. (2015). Variability patterns of the general circulation and sea water temperature in the North Sea. *Progress in Oceanography*, *135*, 91–112.
- Mathis, M., Elizalde, A., & Mikolajewicz, U. (2017). Which complexity of regional climate system models is essential for downscaling anthropogenic climate change in the Northwest European shelf? *Climate Dynamics*, *50*, 1–23.
- Mikolajewicz, U., Gröger, M., Maier-Reimer, E., Schurgers, G., Vizcaino, M., & Winguth, A. M. (2007). Long-term effects of anthropogenic CO₂ emissions simulated with a complex Earth system model. *Climate Dynamics*, *28*(6), 599–633.
- Miller, P. I., & Christodoulou, S. (2014). Frequent locations of oceanic fronts as an indicator of pelagic diversity: application to marine protected areas and renewables. *Marine Policy*, *45*, 318–329.
- Myers, L., & Bahaj, A. (2010). Experimental analysis of the flow field around horizontal axis tidal turbines by use of scale mesh disk rotor simulators. *Ocean Engineering*, *37*(2–3), 218–227.
- Neill, S. P., Hashemi, M. R., & Lewis, M. J. (2014). Optimal phasing of the European tidal stream resource using the greedy algorithm with penalty function. *Energy*, *73*, 997–1006.
- Neill, S. P., Hashemi, M. R., & Lewis, M. J. (2016). Tidal energy leasing and tidal phasing. *Renewable Energy*, *85*, 580–587.
- Neill, S. P., Vögler, A., Goward-Brown, A. J., Baston, S., Lewis, M. J., Gillibrand, P. A., et al. (2017). The wave and tidal resource of Scotland. *Renewable Energy*, *114*, 3–17.
- Ocean Energy Systems (2016). 2016 Annual Report, The Executive Committee of Ocean Energy Systems.
- O'Dea, E., Arnold, A., Edwards, K., Furner, R., Hyder, P., Martin, M., et al. (2012). An operational ocean forecast system incorporating NEMO and SST data assimilation for the tidally driven European North-West shelf. *Journal of Operational Oceanography*, *5*(1), 3–17.
- O'Hara Murray, R., & Gallego, A. (2017). A modelling study of the tidal stream resource of the Pentland Firth, Scotland. *Renewable Energy*, *102*, 326–340.
- OSPAR Commission (2000). Quality Status Report 2000, Region II – Greater North Sea. OSPAR Commission, London.
- Pelling, H. E., Green, J. M., & Ward, S. L. (2013). Modelling tides and sea-level rise: To flood or not to flood. *Ocean Modelling*, *63*, 21–29.
- Pickering, M., Wells, N., Horsburgh, K., & Green, J. (2012). The impact of future sea-level rise on the European shelf tides. *Continental Shelf Research*, *35*, 1–15.
- Pickering, M., Horsburgh, K., Blundell, J., Hirschi, J.-M., Nicholls, R., Verlaan, M., & Wells, N. (2017). The impact of future sea-level rise on the global tides. *Continental Shelf Research*, *142*, 50–68.
- Pingree, R., & Griffiths, D. (1978). Tidal fronts on the shelf seas around the British Isles. *Journal of Geophysical Research*, *83*(C9), 4615–4622.
- Polagye, B., & Thomson, J. (2013). Tidal energy resource characterization: Methodology and field study in Admiralty Inlet, Puget Sound, WA (USA). *Proceedings of the Institution of Mechanical Engineers, Part A: Journal of Power and Energy*, *227*(3), 352–367.
- Pugh, D. T. (1996). *Tides, surges and mean sea-level (reprinted with corrections)*. Chichester, UK: John Wiley.
- Quante, M., Colijn, F., Bakker, J. P., Härdtle, W., Heinrich, H., Lefebvre, C., et al. (2016). Introduction to the assessment - Characteristic of the region, North Sea region climate change assessment (pp. 1–52). Springer.
- Robins, P. E., Neill, S. P., Lewis, M. J., & Ward, S. L. (2015). Characterising the spatial and temporal variability of the tidal-stream energy resource over the Northwest European shelf seas. *Applied Energy*, *147*, 510–522.
- Robinson, I. (1979). The tidal dynamics of the Irish and Celtic Seas. *Geophysical Journal International*, *56*(1), 159–197.
- Sadykova, D., Scott, B., De Dominicis, M., Wakelin, S., Sadykov, A., & Wolf, J. (2017). Bayesian joint models with INLA exploring marine mobile predator-prey and competitor species habitat overlap. *Ecology and Evolution*, *7*(14), 5212–5226.
- Schrum, C., Lowe, J., Meier, H. M., Grabemann, I., Holt, J., Mathis, M., et al. (2016). Projected Change—North Sea. In *North Sea region climate change assessment* (pp. 175–217). Springer.
- Scott, B., Sharples, J., Ross, O. N., Wang, J., Pierce, G. J., & Camphuysen, C. (2010). Sub-surface hotspots in shallow seas: Fine-scale limited locations of top predator foraging habitat indicated by tidal mixing and sub-surface chlorophyll. *Marine Ecology Progress Series*, *408*, 207–226.
- Scott, B., Webb, A., Palmer, M., Embling, C., & Sharples, J. (2013). Fine scale bio-physical oceanographic characteristics predict the foraging occurrence of contrasting seabird species; Gannet (*Morus bassanus*) and storm petrel (*Hydrobates pelagicus*). *Progress in Oceanography*, *117*, 118–129.
- Simpson, J., & Bowers, D. (1981). Models of stratification and frontal movement in shelf seas. *Deep Sea Research Part A. Oceanographic Research Papers*, *28*(7), 727–738.
- Simpson, J., & Rippeth, T. (1993). The Clyde Sea: A model of the seasonal cycle of stratification and mixing. *Estuarine, Coastal and Shelf Science*, *37*(2), 129–144.
- Solomon, S., Qin, D., Manning, M., Chen, Z., Marquis, M., Averyt, K., et al. (2007). *Climate change 2007: The Physical Science Basis. Contribution of Working Group I to the Fourth Assessment Report of the Intergovernmental Panel on Climate Change*. Cambridge, UK and New York: Cambridge University Press.
- Stocker, T. F., Qin, D., Plattner, G.-K., Tignor, M., Allen, S. K., Boschung, J., et al. (2013). *Climate change 2013: The Physical Science Basis. Contribution of Working Group I to the Fifth Assessment Report of the Intergovernmental Panel on Climate Change*. Cambridge, UK and New York: Cambridge University Press.
- Sündermann, J., & Pohlmann, T. (2011). A brief analysis of North Sea physics. *Oceanologia*, *53*(3), 663–689.
- Taylor, K. E., Stouffer, R. J., & Meehl, G. A. (2012). An overview of CMIP5 and the experiment design. *Bulletin of the American Meteorological Society*, *93*(4), 485–498.
- The Crown Estate (2013). *Pentland Firth and Orkney Waters strategic area review project*. London: The Crown Estate, Edinburgh.
- The HadGEM2 Development Team, Martin, G. M., Bellouin, N., Collins, W. J., Culverwell, I. D., Halloran, P. R., et al. (2011). The HadGEM2 family of Met Office unified model climate configurations. *Geoscientific Model Development*, *4*(3), 723–757.
- The Scottish Government (2015). *Scotland's National Marine Plan-A Single Framework for Managing Our Seas*. The Scottish Government, Edinburgh.

- Tinker, J., Lowe, J., Pardaens, A., Holt, J., & Barciela, R. (2016). Uncertainty in climate projections for the 21st century Northwest European shelf seas. *Progress in Oceanography*, *148*, 56–73.
- Turrell, W., Henderson, E., Slesser, G., Payne, R., & Adams, R. (1992). Seasonal changes in the circulation of the northern North Sea. *Continental Shelf Research*, *12*(2), 257–286.
- van der Molen, J., Ruurdij, P., & Greenwood, N. (2016). Potential environmental impact of tidal energy extraction in the Pentland Firth at large spatial scales: Results of a biogeochemical model. *Biogeosciences*, *13*, 2593–2609.
- van Gennip, S. J., Popova, E. E., Yool, A., Pecl, G. T., Hobday, A. J., & Sorte, C. J. B. (2017). Going with the flow: The role of ocean circulation in global marine ecosystems under a changing climate. *Global Change Biology*, *23*(7), 2602–2617.
- Wakelin, S. L., Artioli, Y., Butenschön, M., Allen, J. I., & Holt, J. T. (2015). Modelling the combined impacts of climate change and direct anthropogenic drivers on the ecosystem of the Northwest European continental shelf. *Journal of Marine Systems*, *152*, 51–63.
- Ward, S. L., Green, J. M., & Pelling, H. E. (2012). Tides, sea-level rise and tidal power extraction on the European shelf. *Ocean Dynamics*, *62*(8), 1153–1167.
- Wolf, J., Yates, N., Brereton, A., Buckland, H., De Dominicis, M., Gallego, A., & O'Hara Murray, R. (2016). The Scottish Shelf Model. Part 1: Shelf-wide domain. *Scottish Marine and Freshwater Science*, *7*(3), 151.
- Yang, Z., Wang, T., & Copping, A. E. (2013). Modeling tidal stream energy extraction and its effects on transport processes in a tidal channel and bay system using a three-dimensional coastal ocean model. *Renewable Energy*, *50*, 605–613.
- Zappa, G., Shaffrey, L. C., & Hodges, K. I. (2013). The ability of CMIP5 models to simulate North Atlantic extratropical cyclones. *Journal of Climate*, *26*(15), 5379–5396.
- Zhou, Z., Benbouzid, M., Charpentier, J.-F., Sculler, F., & Tang, T. (2017). Developments in large marine current turbine technologies—A review. *Renewable and Sustainable Energy Reviews*, *71*, 852–858.